ornl

ORNL/MIT-303

OAK
RIDGE
NATIONAL
LABORATORY

UNION
CARBIDE

Reaction Modeling of an Atmospheric Fluidized-Bed Coal Combustor

J. S. Sood
S. K. Fok
J. H. Friedman

OPERATED BY
UNION CARBIDE CORPORATION
FOR THE UNITED STATES
DEPARTMENT OF ENERGY

Printed in the United States of America. Available from
National Technical Information Service
U.S. Department of Commerce
5285 Port Royal Road, Springfield, Virginia 22161
NTIS price codes—Printed Copy: A04; Microfiche A01

ORNL/MIT-303

Contract No. W-7405-eng-26

EMPLOYEE RELATIONS DIVISION

REACTION MODELING OF AN ATMOSPHERIC FLUIDIZED-BED COAL COMBUSTOR

J.S. Sood
S.K. Fok
J.H. Friedman

Consultant:
A.A. Khan

Date Published - June 1980

Oak Ridge Station
School of Chemical Engineering Practice
Massachusetts Institute of Technology
K.J. Fallon, Director

Oak Ridge National Laboratory
Oak Ridge, Tennessee 37830
Operated by
Union Carbide Corporation
for the
Department of Energy

ABSTRACT

A model of an atmospheric fluidized-bed combustor of coal was developed to account for combustion in both the bubbling-bed and freeboard regions. The bubbling bed was modeled by the method of Louis and Tung, while the freeboard model assumed undispersed gas and solid phases. Comparison of feed, bed, and elutriant particle-size distributions obtained from the model indicated realistic qualitative predictions. Parametric sensitivity analyses with respect to bed temperature, superficial velocity, and coal feed rate indicated physically realistic trends. Inclusion of the freeboard region slightly increased predicted combustion efficiencies but led to values which exceeded those reported from the Babcock and Wilcox facility. On the other hand, the model underpredicted those values when the freeboard was excluded. The main weakness of the present model results from dependent inputs which must be calculated *a priori* to maintain consistency.

Contents

1. INTRODUCTION

Atmospheric fluidized-bed combustors (AFBC's) of coal are being recognized as attractive alternatives to conventional boilers. Due to high heat-generation rates and high heat-transfer coefficients, these reactors are energetically efficient. In addition, high-sulfur coals can be burned without unacceptable SO_2 emissions by controlling the loading of limestone or dolomite, while NO_x formation is inhibited by the low temperature of combustion (4). The low requirement of excess air is a further advantage. In view of these merits, significant effort is being directed toward bringing this technology to commercial application.

The AFBC consists primarily of a reactor vessel and auxiliary equipment for the recycle of fines (Fig. 1). Water is passed through heat exchangers to produce steam in both the bed and freeboard region of the combustor. Crushed, screened coal and limestone are pneumatically conveyed in air to the bottom of the vessel. Preheated air in excess of stoichiometric amount is blown through a bubble-cap distributor to fluidize the solid particles.

The combustion chamber may be divided into three regions corresponding to different hydrodynamic regimes. In the "grid" region at the base of the reactor, the volatile matter near the surface of the coal particles is burned rapidly. The bubbling bed is formed above the grid where a dense emulsion phase is agitated by the rising bubbles. Most combustion of carbon is believed to occur in this region. As coal particles become smaller, their transport velocity becomes less than the superficial velocity of the air, and they are elutriated into the 'freeboard' region. Solids may also leave the bed by overflow. Any solids which are not consumed in the freeboard are separated from the flue gas by a cyclone separator and are then recycled for further combustion.

Previous studies of AFBC's have included sophisticated models developed by the MIT Energy Laboratory (6) and Oak Ridge National Laboratory (unpublished work). Most models neglect combustion in the freeboard, although a recent study by Yates and Rowe indicated the importance of this region in fluidized catalytic processes (9). It was suggested to the authors that the contribution of the freeboard to the overall performance of an AFBC might also be quite significant (3). Therefore the objective of this project was to develop a simple model which considered combustion in both the bubbling-bed and the freeboard regions.

The approach taken is summarized by the flow diagram in Fig. 2. First, a submodel was formulated to calculate combustion efficiency in the bubbling-bed region from specified input data. Another submodel was then formulated for the freeboard, and the two were incorporated to predict the overall combustion efficiency of the AFBC. Sensitivity analyses were conducted on both the bubbling-bed and the overall models to assess behavior with respect to selected input parameters. Predicted results were compared with experimental data from the Babcock and Wilcox 6'x6' pilot facility (1).

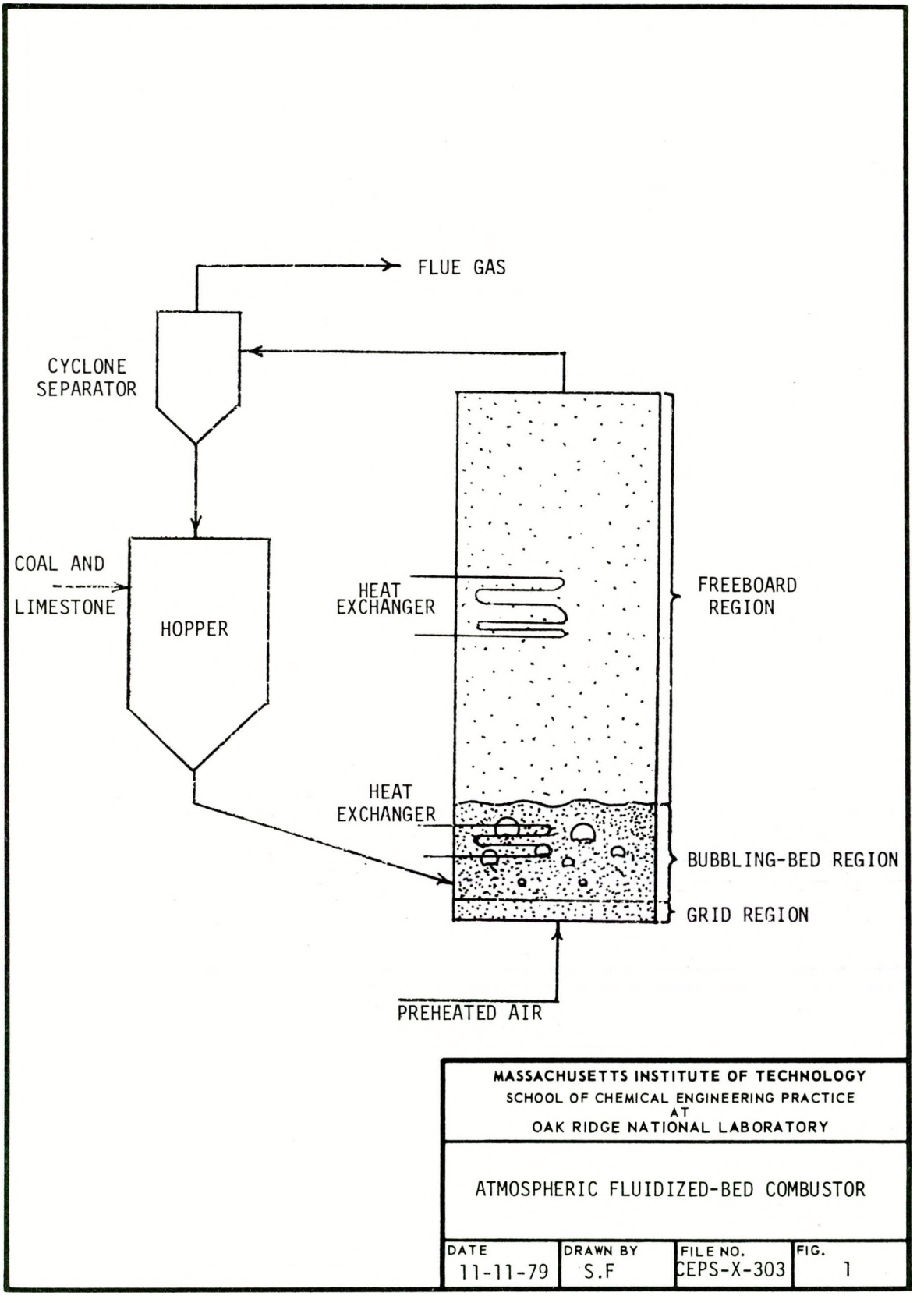
FLUE GAS
CYCLONE SEPARATOR
COAL AND LIMESTONE
HOPPER
HEAT EXCHANGER
FREEBOARD REGION
HEAT EXCHANGER
BUBBLING-BED REGION
GRID REGION
PREHEATED AIR
MASSACHUSETTS INSTITUTE OF TECHNOLOGY
SCHOOL OF CHEMICAL ENGINEERING PRACTICE
AT
OAK RIDGE NATIONAL LABORATORY
ATMOSPHERIC FLUIDIZED-BED COMBUSTOR
DATE 11-11-79
DRAWN BY S.F
FILE NO. CEPS-X-303
FIG. 1

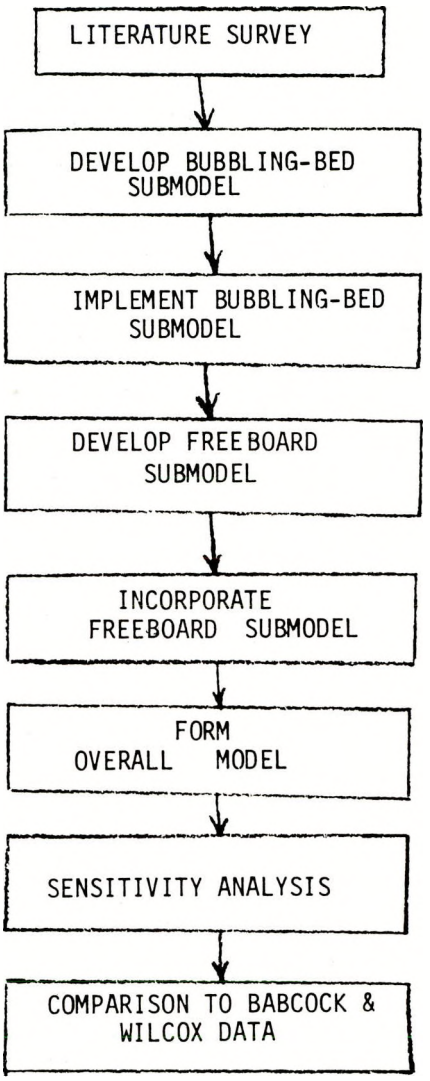

MASSACHUSETTS INSTITUTE OF TECHNOLOGY
SCHOOL OF CHEMICAL ENGINEERING PRACTICE
AT
OAK RIDGE NATIONAL LABORATORY

FLOWCHART OF THE METHOD OF APPROACH

DATE	DRAWN BY	FILE NO.	FIG.
11-27-79	S.F.	CEPS-X-303	2

2. MODEL OF THE FLUIDIZED-BED COMBUSTOR

2.1 Overall Structure of the AFBC Model

A conceptual model of the AFBC is presented in stages for the bubbling-bed and freeboard regions (Fig. 3). The major input parameters included characteristics of the solid and air feeds (Table 1 in Sect. 2.2), while the outputs from the model primarily included characterization of solids in both the overflow and the flue-gas streams. From these parameters, the combustion efficiency was calculated.

For simplicity, the recycle of fines was ignored. In addition, many simplifying assumptions were made for the hydrodynamics in the combustor. These are explained in the following sections.

2.2 Bubbling-Bed-Region Submodel

We based the bubbling-bed submodel on the work of Louis and Tung (6), who modeled this region as two phases. Bubbles which rise through the bed and agitate the emulsion phases were assumed to be in plug flow, while the emulsion phase itself was treated as a continuous stirred tank. The growing bubbles were approximated by an intermediate bubble size of diameter equal to the tube spacing of the heat exchanger. Since all coal particles are in the dense phase and since previous investigators believe that combustion occurs primarily at the surface of the particles (2), we assumed that the combustion reaction occurred only in the emulsion phase.

The interactions of all the physical phenomena considered in this model are illustrated in Fig. 4. At the center of the bubbling-bed submodel is the mass balance proposed by Kunii and Levenspiel, who treated particle shrinkage over a wide particle-size distribution of feed (5). The overall mass balance accounts for coal burned in the bed, transported in the overflow, and carried over by elutriation. A differential mass balance which accounts for shrinkage in and out of particle-size intervals is integrated over the particle-size distribution and is incorporated into the overall mass balance.

Correlations from the literature were used to model particle-size distribution, particle shrinkage, and elutriation. A modified Rosin-Rammler distribution function (8) was fitted to sieve-analysis data of Babcock and Wilcox (1), which contained a wide range of particle sizes to characterize the coal feed (see Appendix 7.3.1). Particle shrinkage depends on both attrition and combustion. Attrition can result from thermal effects as well as from collisions of particles with one another and with heat-exchanger tubes. The phenomena were modeled by using a Merrick-Highley correlation (see Appendix 7.1). The rate of combustion is a function of the oxygen concentration in the emulsion phase, the rate of oxygen diffusion to the surface of the particle, and the rate of surface

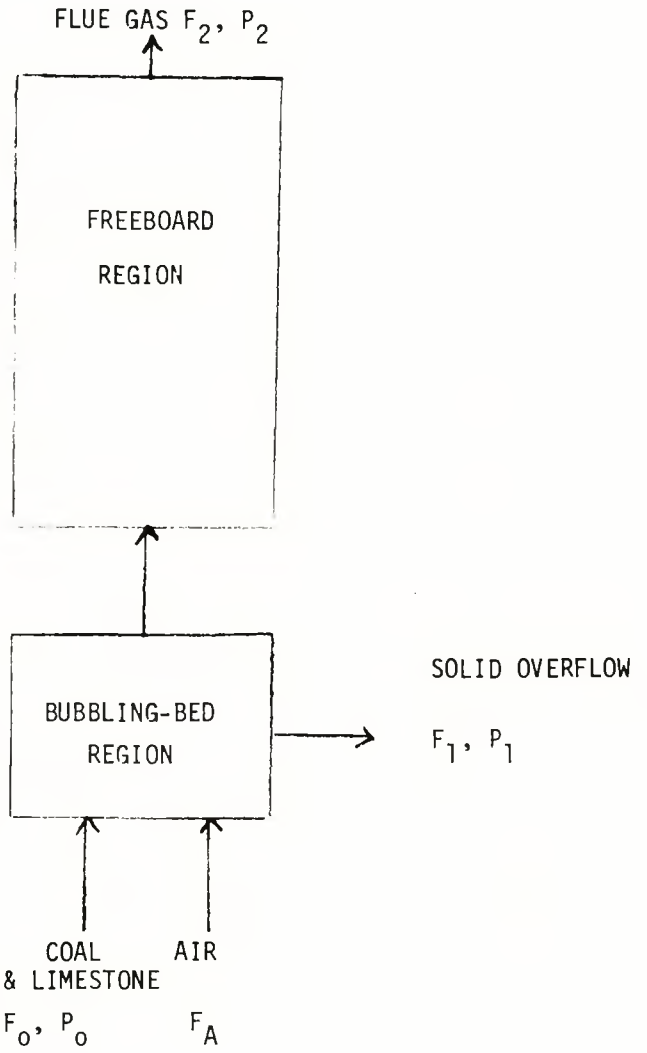

MASSACHUSETTS INSTITUTE OF TECHNOLOGY
SCHOOL OF CHEMICAL ENGINEERING PRACTICE
AT
OAK RIDGE NATIONAL LABORATORY

SCHEMATIC REPRESENTATION OF
ATMOSPHERIC FLUIDIZED-BED MODEL

DATE	DRAWN BY	FILE NO.	FIG.
11-27-79	S.F.	CEPS-X-303	3

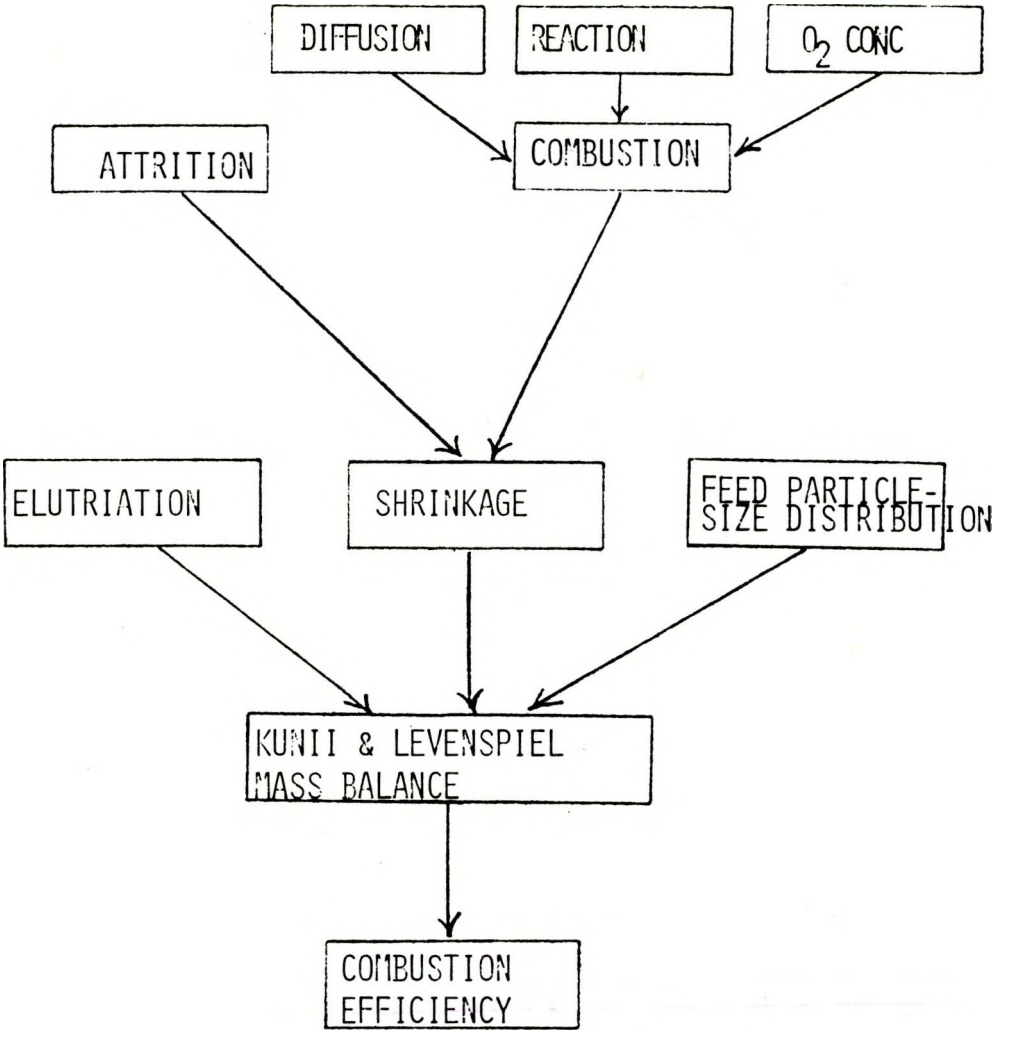

MASSACHUSETTS INSTITUTE OF TECHNOLOGY
SCHOOL OF CHEMICAL ENGINEERING PRACTICE
AT
OAK RIDGE NATIONAL LABORATORY

OVERALL STRUCTURE OF THE BUBBLING-BED SUBMODEL

DATE	DRAWN BY	FILE NO.	FIG.
11-15-79	S.F	CEPS-X-303	4

reaction. Beer (3) developed an expression for shrinkage rate which we incorporated into the present model. Elutriation occurs when the required transport velocity of the shrinking particle becomes less than the superficial gas velocity. We also used the Merrick-Highley (7) correlation to treat this process (Appendix 7.1).

The inputs and outputs of the bubbling-bed submodel are listed in Table 1. Detailed calculations of the input parameters, which may be found in Appendix 7.3.2, correspond to Babcock and Wilcox pilot-plant operation.

Table 1. Input and Output Parameters of the Bubbling-Bed Submodel

Inputs:	bed dimensions
	coal feed rate and size distribution
	coal composition
	air feed rate
	air superficial velocity
	bed temperature
	physical properties of coal and gas
Outputs:	elutriant particle-size distribution
	overflow rate

2.3 Freeboard Submodel

The extent of the combustion of the coal particles elutriated from the bubbling bed is calculated in the freeboard submodel. The inputs and outputs of the submodel are shown in Table 2, and a detailed derivation of the mathematics is given in Appendix 7.2.

Table 2. Input and Output Parameters of the Freeboard Submodel

Inputs:	elutriant particle-size distribution
	physical properties of coal and gas
	coal composition
	bed temperature
	temperature at freeboard heat exchanger
	freeboard dimensions
Outputs:	extent of combustion in the freeboard

We assumed that all particles in the freeboard were transported without backmixing at the same velocity. The oxygen concentration can be considered

constant, because the volume of gas in the freeboard is large relative to the amount of combustion occurring there. The particle-combustion model is identical to the one used in the bubbling-bed region (Appendix 7.1). The rate of particle shrinkage is considered only as a function of temperature, oxygen concentration, and particle radius. These parameters can describe the particle in the freeboard environment as well as in the emulsion phase of the bubbling bed. Because the number of particles in the freeboard is low relative to the volume, there is little interaction between particles,and attrition may be neglected. The interaction between the segments of the freeboard submodel are shown in Fig. 5.

3. RESULTS AND DISCUSSION

3.1 Model Predictions of Particle-Size Distributions

By using the input data shown in Table 3, model predictions of bed and elutriant particle-size distributions were compared,with the feed distribution (Fig. 6). The feed contained a wide distribution with an average particle radius of 431 μm. The bed distribution, with an average radius of 141 μm, was more sharply peaked and skewed toward the y-axis. Elutriated particles were nearly uniform at a radius of 23.5 μm. The results seem physically cogent since particles shrink in the bed until they are elutriated as fines. No experimental data were available to confirm these predictions.

Table 3. Input Parameters - Base Case

Air feed rate	2.264 kg/s
Coal feed rate	1.084 kg/s
Bed height	1.22 m
Bed temperature	1144 K
Superficial velocity	2.5 m/s
Excess air	0.18
Void fraction in bed	0.45
Bed weight	3500 kg

In the freeboard region of the model, the mean-particle radius was monitored as a function of height in the freeboard (Fig. 7). The mean-particle size was reduced dramatically with height, which indicated that the freeboard significantly contributed to particle shrinkage.

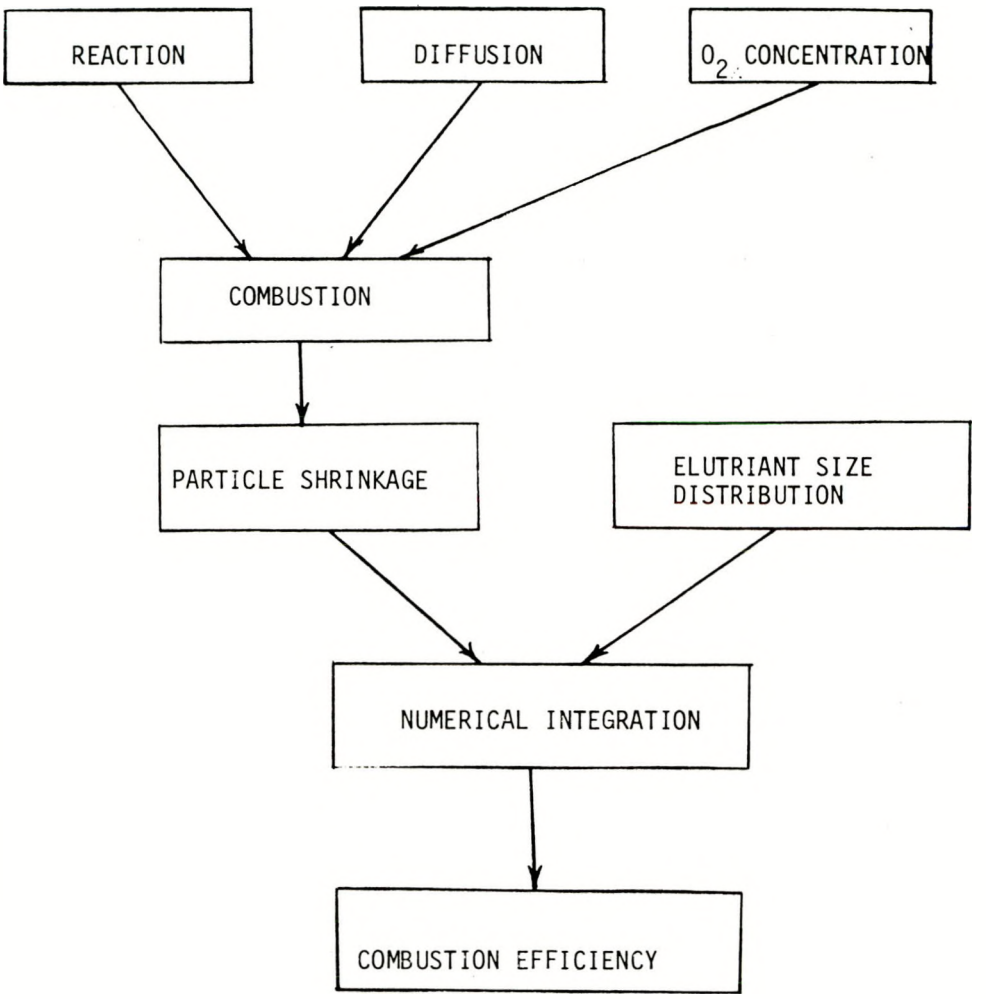

MASSACHUSETTS INSTITUTE OF TECHNOLOGY
SCHOOL OF CHEMICAL ENGINEERING PRACTICE
AT
OAK RIDGE NATIONAL LABORATORY

SCHEMATIC OF FREEBOARD SUBMODEL

DATE	DRAWN BY	FILE NO.	FIG.
11-26-79	SF/JS	CEPS-X-303	5

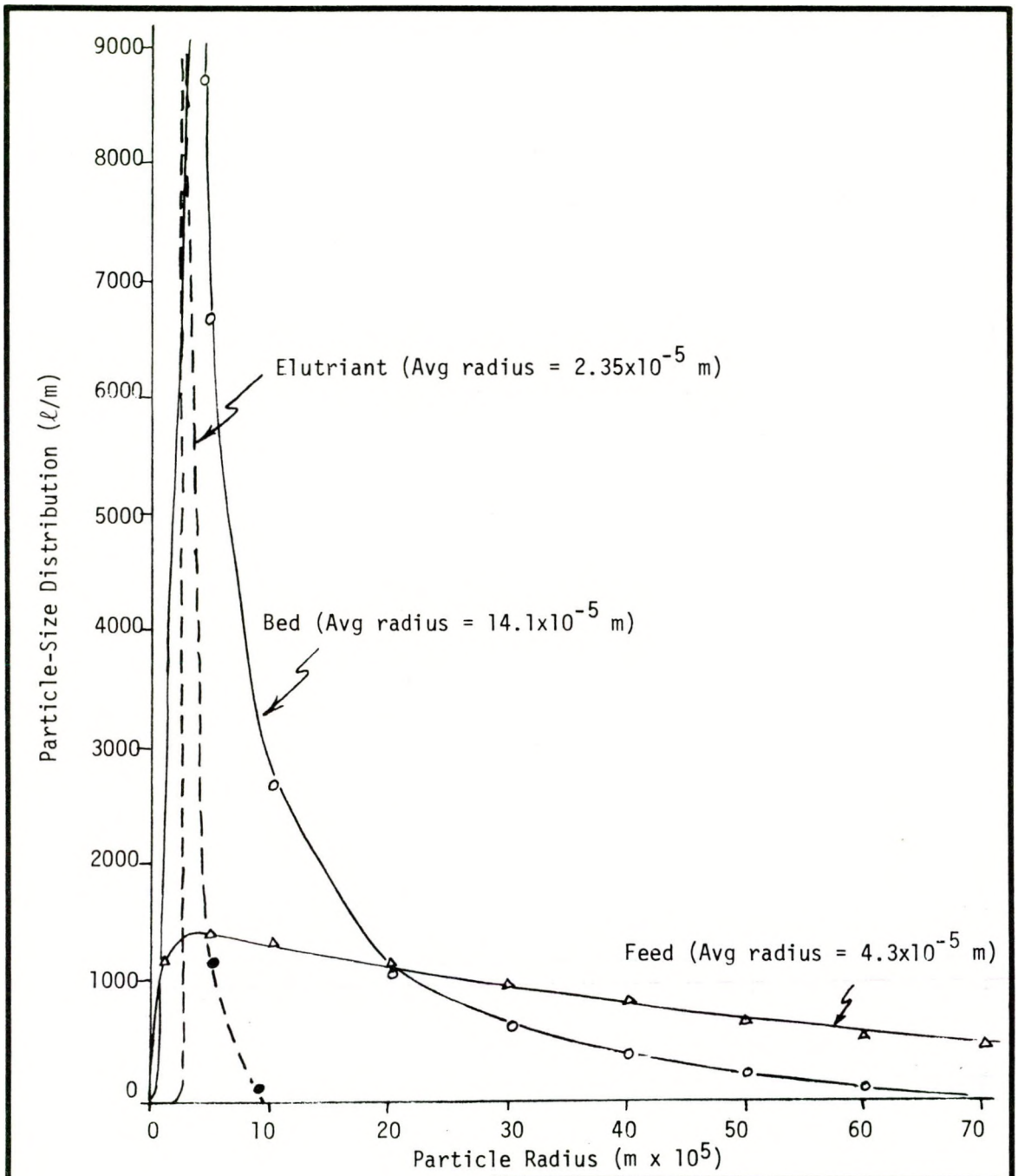

MASSACHUSETTS INSTITUTE OF TECHNOLOGY
SCHOOL OF CHEMICAL ENGINEERING PRACTICE
AT
OAK RIDGE NATIONAL LABORATORY

COMPARISON OF PARTICLE-SIZE DISTRIBUTIONS CALCULATED FROM MODEL

DATE	DRAWN BY	FILE NO.	FIG.
11-26-79	JS	CEPS-X-303	6

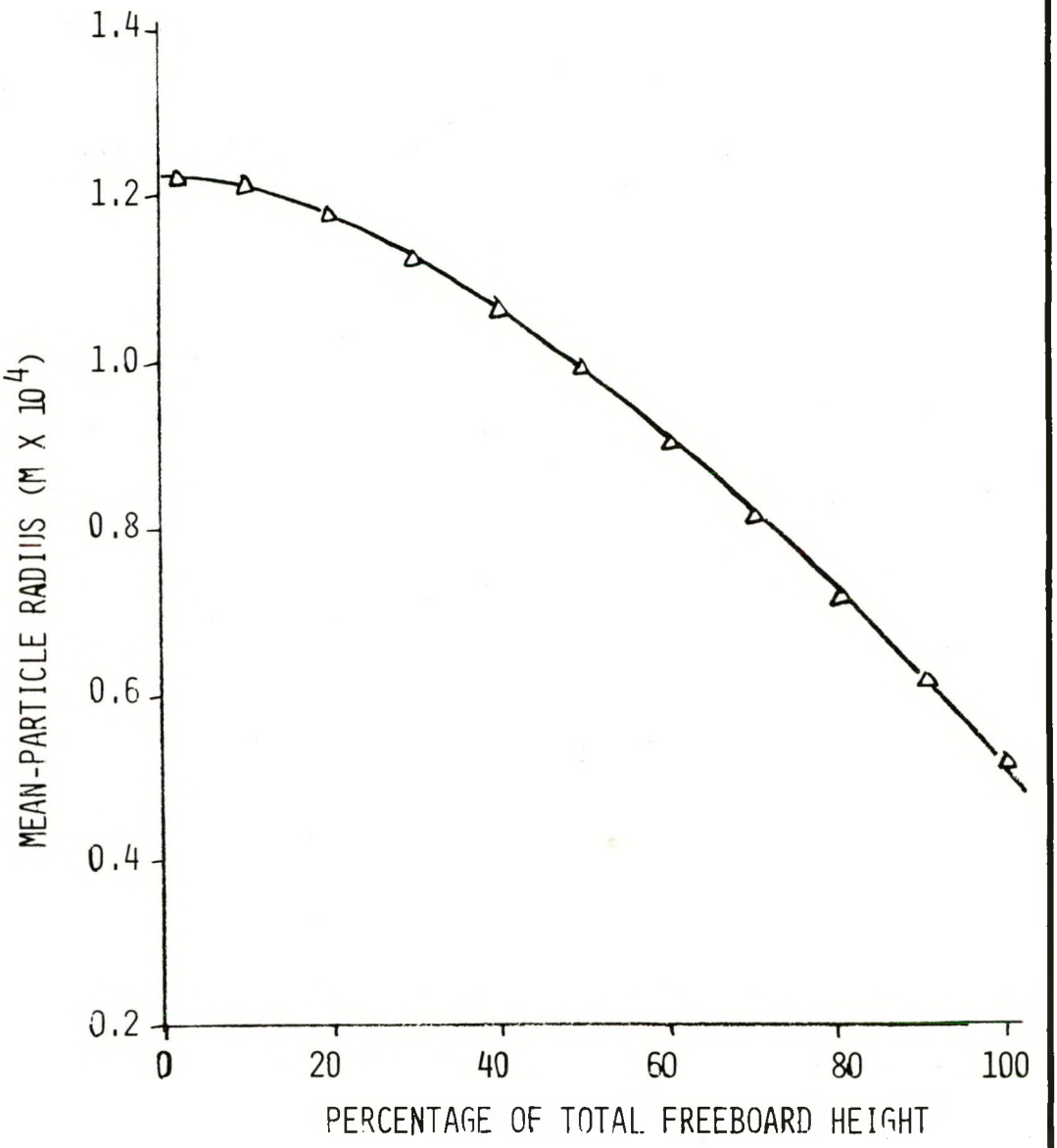

MASSACHUSETTS INSTITUTE OF TECHNOLOGY
SCHOOL OF CHEMICAL ENGINEERING PRACTICE
AT
OAK RIDGE NATIONAL LABORATORY

MEAN-PARTICLE RADIUS VERSUS PERCENTAGE FREEBOARD HEIGHT

DATE	DRAWN BY	FILE NO.	FIG.
11-26-79	S.F.	CEPS-X-303	7

3.2 Sensitivity Analysis

The combustion efficiency predicted by the model was tested for sensitivity with respect to three input parameters: gas temperature, gas superficial velocity, and coal feed rate. Input parameters which were representative of the Babcock and Wilcox combustor operation were selected for a base case around which the test parameters were individually varied. All cases were run both with and without the freeboard submodel to isolate its effects on the combustion efficiency prediction. Experimental data from Babcock and Wilcox pilot plant (1) were compared with the model predictions.

The present structure of the model does not guarantee internal consistency because it is possible to specify physically intractable combinations of inputs. The interdependencies of input parameters for which the model does not account are shown in Table 4. For the sensitivity analysis, input parameters were varied in ranges where the interactions should not seriously affect model performance. Coal feed rate is the most independent parameter. The superficial velocity only shows the relative influence of the freeboard model; an absolute comparison of the curves may not be valid because u_0 was varied independently. Finally, the insensitivity of the model to temperature suggests the need to account for input interactions.

Table 4. Input Parameter Interaction Not Considered in Model

	Volumetric Air Flow Rate	Expanded Bed Height	Gas Temperature	Molar Density of Incoming Air
Volumetric air flow rate		x		
Gas temperature		x		x
Mass density of incoming air			x	x
Gas diffusivity			x	
Gas viscosity			x	
Superficial velocity	x	x	x	x
Amount of excess air	x			
Height of freeboard		x		

The sensitivity of combustion efficiency to gas temperature, which was varied between 1000 and 1300 K, is shown in Fig. 8. Without the inclusion of combustion in the freeboard, a slight linear increase in efficiency was approximately constant at 0.943. Higher temperatures decrease

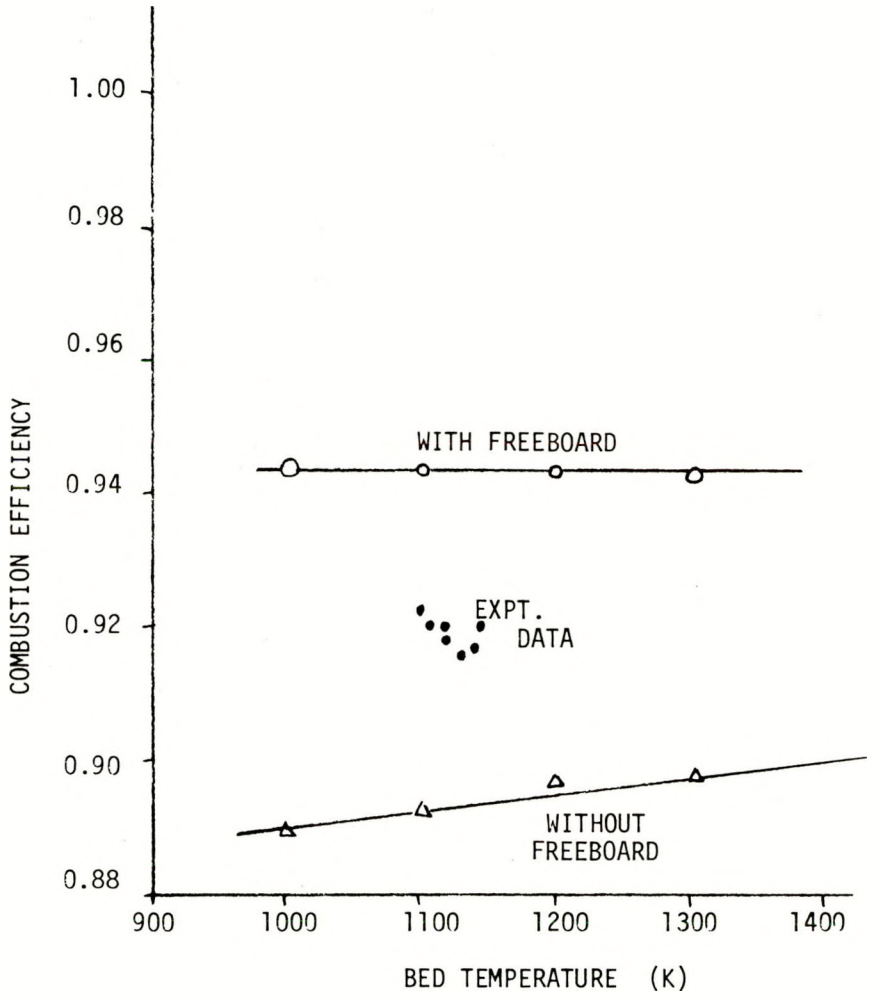

(Operating Conditions given in Table 3.)

MASSACHUSETTS INSTITUTE OF TECHNOLOGY SCHOOL OF CHEMICAL ENGINEERING PRACTICE AT OAK RIDGE NATIONAL LABORATORY			
COMBUSTION EFFICIENCY AS A FUNCTION OF BED TEMPERATURE			
DATE 11-25-79	DRAWN BY S.F/ H.F	FILE NO. CEPS-X-303	FIG. 8

particle burning time, which decreases elutriation and increases efficiency. The freeboard model has a dampening effect on the elutriation term, which accounts for the nearly constant efficiency with the freeboard.

These variations are very small because the present model only accounts for the kinetic effects of temperature, while it ignores variations in physical properties. For example, increasing temperature and decreasing density will increase superficial velocity, bubble size, and bed height. Elutriation will also increase, with a negative effect on efficiency. However, the larger bed height and bubble size should enhance the available oxygen concentration, which would result in higher efficiency. The net effect on combustion efficiency may be either positive or negative.

The relationship between bed combustion efficiency and superficial velocity is shown in Figure 9. When freeboard combustion was neglected, the model predicted a sharp drop in efficiency with increasing velocity, as would be expected, since elutriation varies directly with superficial velocity. However, inclusion of the freeboard model resulted in a linear increase in efficiency. The highly efficient model for freeboard combustion simulated burning above the bed of most of the elutriant. Higher superficial velocity also reduces carbon loading in the bed, which increases efficiency. Thus, the net effect on combustion efficiency is positive rather than negative. This result may indicate that the freeboard combustion model is too efficient.

Freeboard combustion increased total combustion by about 4% over the entire range of coal feed rates introduced to the model (Fig. 10). In addition, the extent of combustion increased with increasing coal feed rates. Solid loading of the bed increases less than proportionately with coal feed rate. Since elutriation and overflow rates are direct functions of carbon loading, they will increase less than proportionally, which causes combustion efficiency to increase. This effect becomes more pronounced at higher feed rates. In practice, these curves would be limited by oxygen availability and bed volumetric capacity. The steeper slope predicted by including the freeboard model is due to highly efficient freeboard combustion; thus, the effect of increased elutriation is counteracted.

The experimental data do not manifest discernible variations since pilot-plant operating parameters were kept relatively constant and combustion efficiency varied over a small range. While our model predictions ranged from 0.60 to 0.94 without the freeboard and 0.89 to 0.99 with the freeboard, the Babcock and Wilcox data fall between 0.94 and 0.97 and consistently between the two model curves. Again, this result may indicate an excessively efficient freeboard routine.

4. CONCLUSIONS

1. Our model predictions of combustion efficiency are close to data obtained from the Babcock and Wilcox pilot plant.

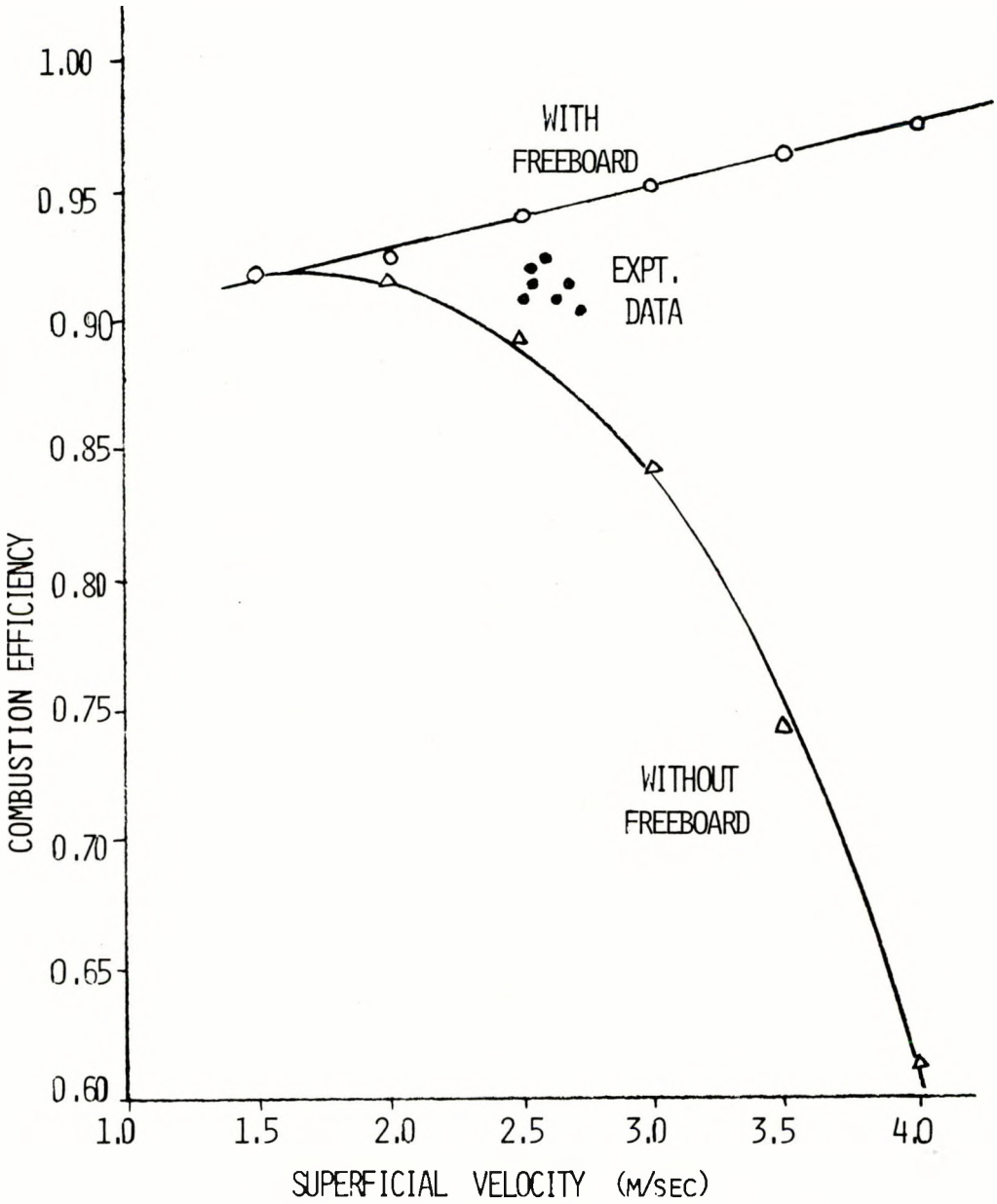

MASSACHUSETTS INSTITUTE OF TECHNOLOGY
SCHOOL OF CHEMICAL ENGINEERING PRACTICE
AT
OAK RIDGE NATIONAL LABORATORY

SUPERFICIAL VELOCITY AS A FUNCTION OF COMBUSTION EFFICIENCY

DATE	DRAWN BY	FILE NO.	FIG.
11-25-79	S.F / H.F	CEPS-X-303	9

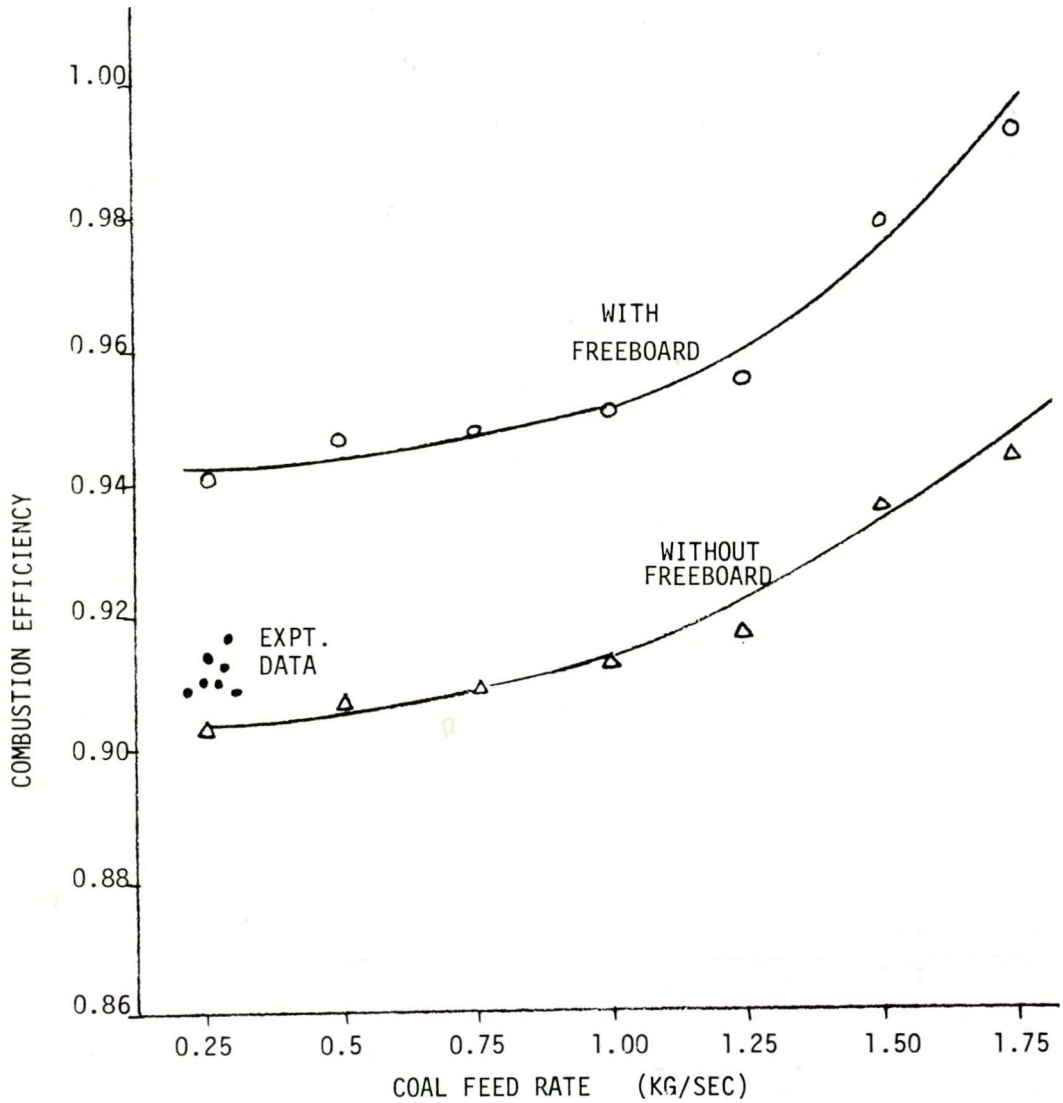

MASSACHUSETTS INSTITUTE OF TECHNOLOGY
SCHOOL OF CHEMICAL ENGINEERING PRACTICE
AT
OAK RIDGE NATIONAL LABORATORY

COMBUSTION EFFICIENCY AS A
FUNCTION OF COAL FEED RATE

DATE	DRAWN BY	FILE NO.	FIG.
11-25-79	S.F/ H.F	CEPS-X-303	10

2. The freeboard model slightly increases the prediction of combustion efficiency.

3. The experimental data lie between predictions made with and without the freeboard. Therefore, the freeboard model efficiency predictions are too high.

4. Calculated changes in efficiency with superficial velocity, bed temperature, and coal feed are physically cogent.

5. RECOMMENDATIONS FOR FUTURE STUDY

1. The model should be modified to provide for interaction of input parameters to prevent over-specification.

2. The model predictions should be compared with those of more complex models. The MIT and ORNL systems are likely candidates for this work.

3. The freeboard submodel should be further refined and tested. The temperature profile and particle combustion mechanism are of particular interest.

4. Model predictions should be compared with more extensive experimental data.

6. ACKNOWLEDGMENTS

We express our gratitude to our consultant, A.A. Khan, for his insight and direction throughout the project. We also acknowledge Profs. Beer and Tung, upon whose work much of our bubbling-bed submodel was based.

7. APPENDIX

7.1 Derivation of Bubbling-Bed Submodel

The interactions between the segments of the bubbling-bed submodel are shown in Fig. 5. The function of this appendix is to provide a mathematical treatment of the segments of the submodel. First, the mass balance of Kunii & Levenspiel is discussed, followed by a discussion of elutriation and particle shrinkage. Finally, combustion efficiency is defined. A discussion of the feed particle-size distribution is treated separately in Appendix 7.3.1.

7.1.1 Mass Balance

The submodel was constructed around the particle-shrinkage model of Kunii & Levenspiel (5). The mass balance was performed on the carbon particles throughout the bed. It consisted of an overall mass balance and an incremental balance on size intervals of coal particles.

The overall mass balance was of the form:

$$F_o = F_1 + F_2 + \text{rate of coal burned in the bed} \qquad (1)$$

where F_o is the solid feed rate (kg/s), F_1 is the solid overflow rate (kg/s), and F_2 is the solid elutriation rate. The incremental mass balance was performed for particles in the radius interval r to r+Δr:

$$F_o p_o(r) - F_1 p_1(r) - WK(r)p_1(r) - W\frac{d[R(r)\ p_1(r)]}{dr} + \frac{3W}{r} p_1(r)\ R(r) = 0 \qquad (2)$$

where

$p_o(r)$ = feed particle-size distribution

$p_1(r)$ = overflow particle-size distribution

W = bed weight, kg

$R(r)$ = shrinkage rate = dr/dt, μm/s

$K(r)$ = elutriation rate constant, kg/m^2-s

The first three terms of the equation correspond to particles entering the vessel as feed or leaving it by overflow or elutriation. The remaining terms account for net shrinkage from the particle-size interval and particle shrinkage within the interval. Proper manipulation of Eqs. (1) and (2) yields the size distribution and flow rates of the outflow streams.

Louis and Tung (6) present a derivation of the performance equations from the above mass balances. The primary equations are as follows:

$$p_b(r) = \frac{F_o I(r,\infty)}{W|S_t(r)|} \int_r^\infty \frac{p_o(r_o)dr_o}{I(r_o,\infty)} \tag{3}$$

$$\frac{W}{F_o} = \int_o^\infty \frac{I(r,\infty)}{|S_t(r)|}\, dr \int_r^\infty \frac{p_o(r_o)dr_o}{I(r_o,\infty)} \tag{4}$$

where $I(r,r_o)$ is the performance function and is defined according to:

$$I(r,r_o) \equiv \exp\left(- \int_r^{r_o} \frac{\frac{F_1}{W} + K(r) + \frac{[3S_c(r)]}{r}}{|S_t(r)|}\, dr \right) \tag{5}$$

where

$p_b(r)$ = bed particle-size distribution

W = weight of carbon in the bed, kg

$S_c(r)$ = particle shrinkage rate due to combustion, μm/s

$S_t(r)$ = total particle shrinkage rate, μm/s

Equations (3) through (5) formed the basis for the prediction of combustion efficiency.

7.1.2 Elutriation

Elutriation is incorporated into the model through the performance equation derived from the mass balance, Eq. (5). The rate of elutriation of solids of size r is characterized by a net upward flux and can be expressed mathematically as:

$$\left(\begin{array}{c}\text{rate of elutriation of solids} \\ \text{of size r per area of bed}\end{array}\right) = K(r)\left(\begin{array}{c}\text{fraction of bed} \\ \text{particles at size r}\end{array}\right) \tag{6}$$

The Merrick-Highley correlation (7) was used to determine the value of the elutriation constant K(r):

$$K(r) = 130\ F_a \exp\left[-10.4\left(\frac{u_t}{u_o}\right)^{0.5}\left(\frac{u_{mf}}{u_o - u_{mf}}\right)^{0.25}\frac{28.84}{A}\right] \quad (7)$$

where

F_a = air feed flow rate, kg/s

u_t = terminal velocity, m/s

u_o = superficial gas velocity, m/s

u_{mf} = minimum fluidizing gas velocity, m/s

A = cross-sectional bed area, m^2

7.1.3 Particle Shrinkage

Total shrinkage of particles is due to both attrition and combustion:

$$S_t(r) = S_a(r) + S_c(r) \quad (8)$$

The rate of particle shrinkage due to attrition was derived from a correlation presented by Merrick and Highley (7):

$$S_a(r) = \frac{K_a}{3}(u_o - u_{mf})(r) \quad (9)$$

where K_a is the attrition constant.

Shrinkage due to combustion was modeled as a function of the amount of available oxygen, the rate of diffusion of oxygen to the particle surface, and the rate of combustion at the particle surface. The development of the particle shrinkage is taken from Louis and Tung (6).

The particle shrinkage rate is given by:

$$S_c(r) = \frac{dr}{dt} \quad (10)$$

so that the consumption of moles of carbon N is:

$$\frac{dN}{dt} = \frac{\rho_c}{12}(4\pi r^2)\, S_c(r) \qquad (11)$$

where ρ_c is the apparent density of coal. The change in moles can also be expressed by the oxygen that diffuses to the particle surface:

$$\frac{dN}{dt} = 2\pi r\ Sh\ D\ (C_p - C_s) \qquad (12)$$

where Sh is the Sherwood number, D is the diffusivity of oxygen, C is the oxygen concentration in the bulk gas and at the surface. Rearrangement of these expressions yields:

$$S_c(r) = \frac{6\ Sh\ D}{\rho_c r}\, C_p\left(1 - \frac{C_s}{C_p}\right) \qquad (13)$$

If the quantity C_s/C_p is substituted by the kinetic expression,

$$\frac{C_s}{C_p} = \frac{1}{1 + \dfrac{82.06\ K_s r T}{600\ Sh\ D}} \qquad (14)$$

where T is the gas temperature and K_s is the combustion rate constant (g/cm^2-s-kPa). The overall equation describing particle shrinkage due to combustion becomes:

$$S_c(r) = \frac{C_p}{\rho_c}\ \frac{1}{\dfrac{100}{82.06\ K_s\ T} + \dfrac{r}{6\ Sh\ D}} \qquad (15)$$

In this overall expression, K_s is described by an Arrhenius equation:

$$K_s = A_o \exp(-E/RT) \qquad (16)$$

where A_o is a pre-exponential factor (57.3 g/cm^2-s-kPa), and E is the activation energy (37,500 J/mol). The Sherwood number is calculated from an empirical correlation by Ranz and Marshall which considers mass transfer of a component from a fluid to a free-falling solid particle (5):

$$Sh = 2 + 0.6(Re)^{0.5} (Sc)^{0.33} \quad (17)$$

where

$$Re = \text{Reynolds number} = \frac{2r\, u_o\, \rho_m}{\mu}$$

$$Sc = \text{Schmidt number} = \frac{\mu}{\rho_m D}$$

From Eq. (15), the shrinking rate is a direct function of the concentration available in the emulsion phase, C_p. The separate contributions of reaction and diffusion to the shrinking rate are represented by the two terms of the denominator.

Two limiting cases of particle shrinkage can be considered. For particles of radius greater than 100 μm, the shrinking is diffusion-limited and the reaction term in Eq. (15) may be neglected:

$$S_c(r) = \frac{6\, C_p\, D\, Sh}{\rho_c r} \quad (18)$$

For particles of radius less than 50 μm, the reaction at the surface is the rate-limiting mechanism, and Eq. (15) becomes:

$$S_c(r) = \frac{0.82\, C_p\, K_s\, T}{\rho_c} \quad (19)$$

The model primarily uses the expression in Eq. (15), which includes both reaction and diffusion contributions to particle shrinkage.

7.1.4 Combustion Efficiency

The combustion efficiency is the output of interest from the simulation and is defined as the ratio of the rate of coal combusted to the rate of coal feed. From the overall mass balance [Eq. (1)], the rate of combustion may be expressed as:

$$\text{rate of combustion} = F_o - F_1 - F_2 \quad (20)$$

Thus, the combustion efficiency may be described as:

$$\eta_c = \frac{F_o - F_1 - F_2}{F_o} \quad (21)$$

7.2 Derivation of the Freeboard Submodel

The basic plug-flow equation can be applied to any particle entering the freeboard. This takes the form:

$$r_f - r_o = \int_o^{x_f} \left(\frac{dr}{dx}\right) dx \tag{22}$$

where r_f is the particle radius at the exit from the freeboard, r_o is the radius at the entrance, x is the vertical coordinate, and x_f is the freeboard height. If the particles have velocity v,

$$r_f - r_o = \frac{1}{v} \int_o^{x_f} \left(\frac{dr}{dx}\right) dx \tag{23}$$

Averaging the conversion in the freeboard ξ_{fb} over the particle-size distribution entering the freeboard p_e gives:

$$\xi_{fb} = \int_o^{r_{max}} \left(\frac{1}{r_o v} \int_o^{x_f} \left(\frac{dr}{dt}\right) dx + 1 \right) p_e(r_o)\, d(r_o) \tag{24}$$

To calculate the combustion efficiency of the model including the freeboard, the elutriation term F_2 in Eq. (20) is then multiplied by ξ_{fb}:

$$\eta_c = \frac{F_o - F_1 - \xi_{fb} F_2}{F_o} \tag{25}$$

7.3 Input Specification

7.3.1 Feed Particle-Size Distribution

The Rosin-Rammler function was used to model the particle-size distribution of the feed (8). It is defined as:

$$1 - P_o(r) = \exp\left[-\left(\frac{r}{b}\right)^n\right] \tag{26}$$

where b and n are size parameters, and $P_o(r)$ is the weight fraction

of total coal feed of particle size less than r. The size parameters for specific data can be determined from a graph of the corresponding logarithmic equation. The regressional analysis for Ohio #6 coal-sieve data is shown in Table 5.

Table 5. Regressional Analysis of Coal-Sieve Data

Mesh	$P_o(r)$	r (cm)	$\ell n[-\ell n(1 - P_o)]$	$\ell n\ r$
0.25	0.998	0.3175	1.827	-1.14
4	0.961	0.2375	1.177	-1.43
8	0.958	0.1190	1.154	-2.12
16	0.606	0.0595	-0.071	-2.82
30	0.354	0.0297	-0.828	-3.51
50	0.190	0.0149	-1.556	-4.21
100	0.098	0.0074	-2.273	-4.89
200	0.056	0.0044	-2.847	-5.59
325	0.028	0.0022	-3.575	-6.49

The data plotted in Fig. 11 indicated a correlation coefficient of 0.9949, with values for n and b of 1.068 and 0.0599, respectively. A cumulative plot of the data and the Rosin-Rammler correlation obtained from these parameters is presented in Fig. 12.

Differentiation of the cumulative Rosin-Rammler function in Eq. (26) with respect to r yielded the incremental particle-size distribution of the feed:

$$\nu = 100\ n\ \frac{r^{n-1}}{b^n}\ \exp[-(\frac{r}{b})^n] \qquad (27)$$

$$= 2159\ (r^{0.068})\ \exp[-(\frac{r}{0.0599})^{1.068}]$$

where ν = Δwt %/Δradius. A graph of Eq. (27) is presented in Fig. 13. The Rosin-Rammler distribution curve for feed particles gave a reasonably good qualitative depiction of the sieve-analysis data taken from plant samples.

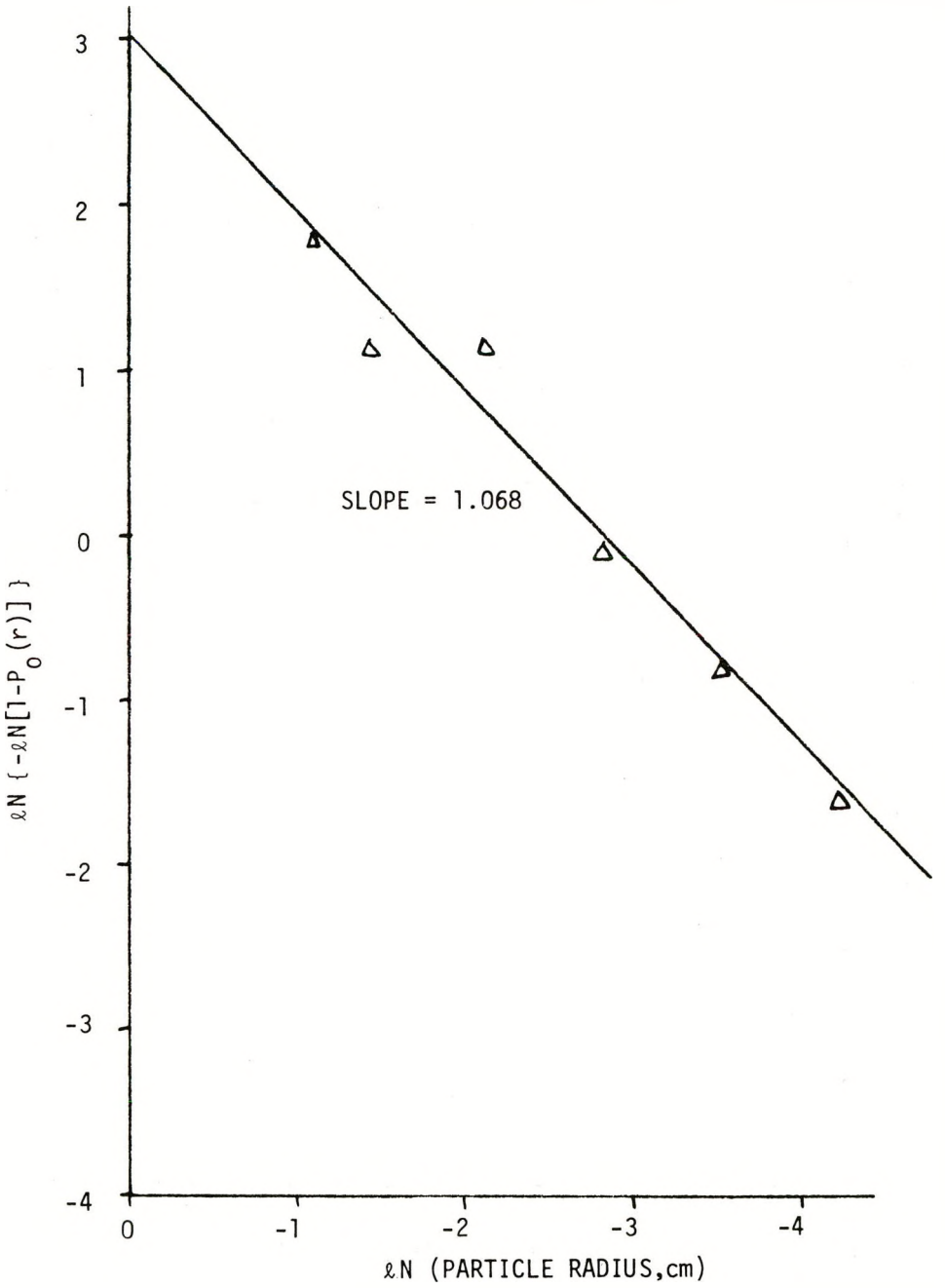

MASSACHUSETTS INSTITUTE OF TECHNOLOGY
SCHOOL OF CHEMICAL ENGINEERING PRACTICE
AT
OAK RIDGE NATIONAL LABORATORY

PLOT FOR EVALUATION OF ROSIN-RAMMLER FUNCTION PARAMETERS

DATE	DRAWN BY	FILE NO.	FIG.
11-15-79	S.F	CEPS-X-303	11

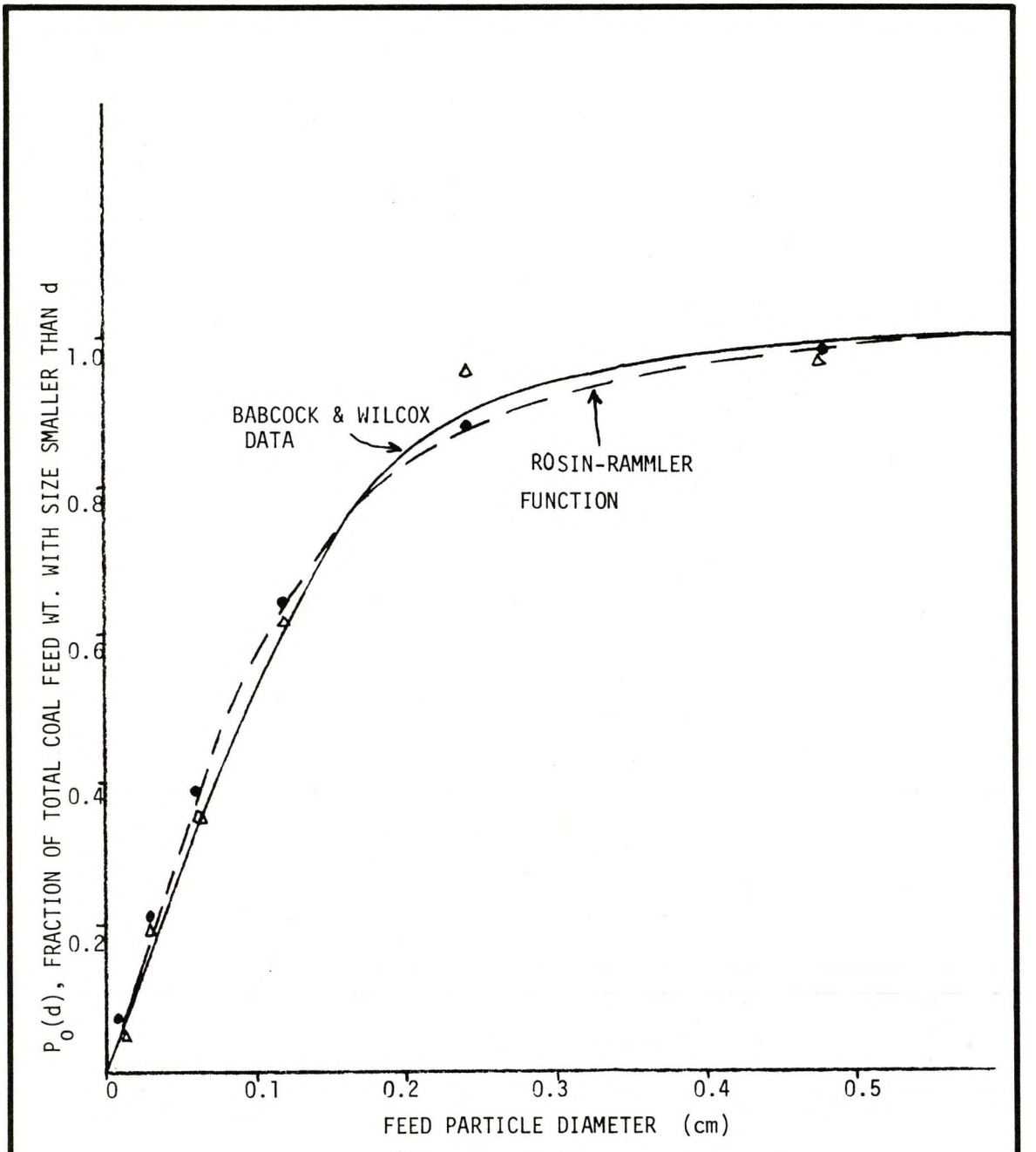

MASSACHUSETTS INSTITUTE OF TECHNOLOGY
SCHOOL OF CHEMICAL ENGINEERING PRACTICE
AT
OAK RIDGE NATIONAL LABORATORY

PARTICLE-SIZE ACCUMULATIVE WEIGHT FRACTION OF COAL FEED, (ROSIN-RAMMLER FUNCTION)

DATE	DRAWN BY	FILE NO.	FIG.
11-15-79	S.F.	CEPS-X-303	12

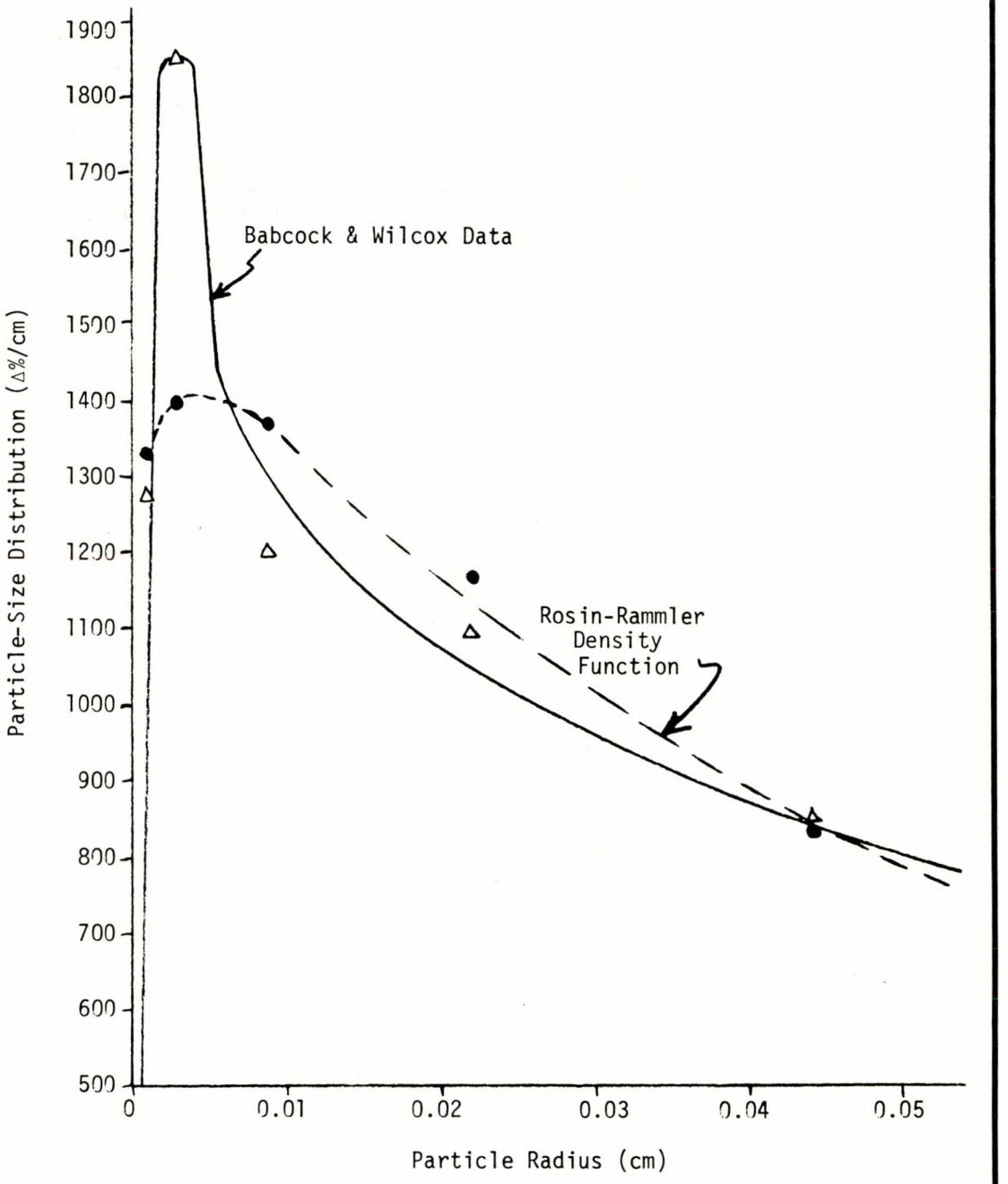

MASSACHUSETTS INSTITUTE OF TECHNOLOGY
SCHOOL OF CHEMICAL ENGINEERING PRACTICE
AT
OAK RIDGE NATIONAL LABORATORY

COAL-FEED PARTICLE-SIZE DISTRIBUTION

DATE	DRAWN BY	FILE NO.	FIG.
11-15-79	S.F	CEPS-X-303	13

7.3.2 Calculation of Other Input Parameters

Estimates of values for the various input parameters were based on two sources. Coal and air feed rates were chosen to be comparable to rates reported by Babcock and Wilcox (1). Values of hydrodynamic properties were calculated as suggested by Louis and Tung (6), although constant values were employed for temperature (1144 K), pressure (1.01 kPa), and feed values of the base case (see Table 3). These calculations are summarized below. The symbols in parenthesis indicate the corresponding variables used in the computer parameter.

7.3.2.1 Diffusivity of Air (DG)

$$DG = (5.187 \times 10^{-4})(T)^{1.5}/P$$

At $P = 1.013 \times 10^5$ Pa and T = 1144 K,

$$DG = \frac{(5.187 \times 10^{-4})(1144)^{1.5}}{1.013 \times 10^5} = 2 \times 10^{-4} \text{ m}^2/\text{s}$$

7.3.2.2 Air Molar Density (RHOM)

$$RHOM = \frac{P}{RT} \text{ (assuming ideal gas)}$$

$$= \frac{1 \text{ atm}}{(82 \text{ atm-cm}^3/\text{gmol-K})(1144 \text{ K})}$$

$$\approx \frac{10^3}{82(1144)} = 1.07 \times 10^{-2} \text{ kg mol/m}^3$$

7.3.2.3 Mass Density of Incoming Air (RHOG)

$$RHOG = RHOM(29 \text{ kg/kg mol}) = (1.07 \times 10^{-2})(29)$$

$$= 0.3094 \text{ kg/m}^3$$

7.3.2.4 Mass Exchange Coefficient Between Bubble and Phase (KBP)

$$KBP = 4.5 \frac{u_{mf}}{d_b} + \frac{5.85(DG)^{1/2}(g)^{1/4}}{(d_b)^{5/4}}$$

where

u_{mf} = minimum fluidization velocity (m/s)

d_b = bubble diameter (m)

DG = diffusivity of O_2 in N_2 (m^2/s)

g = gravitational acceleration (m/s^2)

To estimate u_{mf},

$$u_{mf} = \frac{\sqrt{\beta} - G}{2B}$$

where

$$B = \frac{1.75}{\phi_s \, \varepsilon_{mf}^3} \left(\frac{d_p \rho_g}{\mu}\right)^2$$

$\phi_s \cong 0.65$

$\varepsilon_{mf} \cong 0.45$ = void fraction in emulsion phase

d_p = 2380 μm = acceptor mean particle size

ρ_g = 0.3094 kg/m^3 = mass density of incoming air

$$\mu = \frac{(1.09875 \times 10^{-6}) \, T^{1/2}}{(0.9183 - 9.08 \times 10^{-5} \times T)} = 4.5631 \times 10^{-5} \text{ N-s/m}^2 \text{ at } 1144 \text{ K}$$

$$G = \frac{150(1 - \varepsilon_{mf})}{\phi_s^2 \, \varepsilon_{mf}^3} \left(\frac{d_p \rho_g}{\mu}\right)$$

$\beta = G^2 - 4BC$

$C = -d_p^3 \rho_g (\rho_a - \rho_g) g / \mu^2$

B = 7696.2

G = 34,580

C = -29,904

Therefore,

u_{mf} = 0.7422 m/s

If it is assumed that d_b = 0.122 m, then

$$KBP = 4.5\frac{0.7422}{0.122} + \frac{5.85(2 \times 10^{-4})^{1/2}(9.81)^{1/4}}{(0.122)^{5/4}} = 29.41\ s^{-1}$$

7.3.2.5 Air Flow in Emulsion Phase (EMFLOW)

EMFLOW = (minimum fluidization velocity)(cross-sectional bed area)(air molar density)

= (0.7422 m/s)(3.34 m^2)(kg mol/m^3 0.0107)

= 0.0026 kg mol/s

7.3.2.6 Transport Air Flow Rate (CLFLOW)

CLFLOW = (3800 lb/h)(0.45 kg/lb)(1/3600 h/s)(1/28 kg mol/kg)

= 1.7×10^{-2} kg mol/s

7.3.2.7 Air Flow in Bubble Phase (BUFLOW)

BUFLOW = (air feed rate) + (transport air flow rate) - (air flow rate in emulsion phase)

= (2.3) + (1.7×10^{-2}) - (2.6×10^{-2}) kg mol/s

= 2.29 kg mol/s

7.3.2.8 Weight of Inert in Bed (WEIRT)

WEIRT = (ΔP_{bed})(cross-sectional area of bed)

= 10,458 N/m^2(3.34 m^2)$(\frac{1\ kg}{g\ N})$ = 3.5×10^3 kg

7.4 Computer Program

7.4.1 Program Description

In implementing the model into the PDP-10 computer system, the bubbling-bed and the freeboard region submodels were treated as the subroutines BUBED and FB, respectively. Each subroutine was called from the main program. Initial values of all the input and internal parameters were assigned through a block data subroutine and transmitted between subroutines by COMMON. Detailed calculations of the input parameters are given in Appendix

7.3.2. A flow diagram of the overall program structure is given in Fig. 14. A program listing is given in Appendix 7.4.2.

After the bubbling-bed subroutine divides the empirical correlation of the feed distribution into 60 intervals, the particle shrinkage of each interval is calculated for both combustion and attrition. The major outputs of the subroutine are the particle-size distribution of the elutriated solid and the mass flow rate of the bed overflow (Table 1). The main program then uses these outputs to calculate the combustion efficiency. A detailed flowsheet is shown in Fig. 15 and the listing of subroutine BUBED in Appendix 7.4.2.

The model of the freeboard region is implemented in the subroutine after the effective oxygen concentration, particle velocity, and height increment are calculated. Two nested loops are entered which correspond to the integrals in Eq. (24) (Appendix 7.2.3). The integration subroutine TRAP is used to evaluate the integrals. A flowsheet for the freeboard region model is shown in Fig. 16.

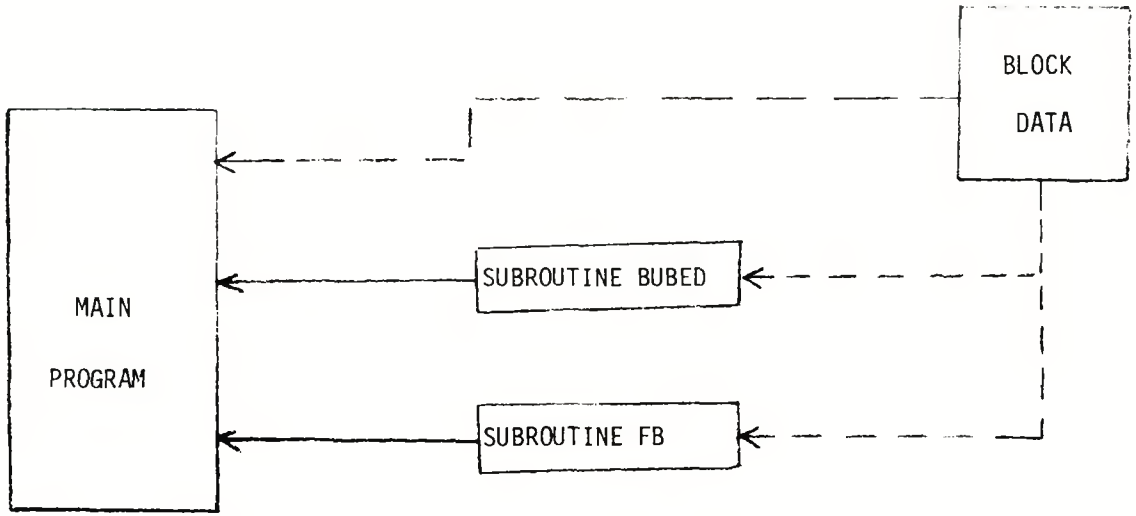

MASSACHUSETTS INSTITUTE OF TECHNOLOGY
SCHOOL OF CHEMICAL ENGINEERING PRACTICE
AT
OAK RIDGE NATIONAL LABORATORY

OVERALL PROGRAM STRUCTURE

DATE	DRAWN BY	FILE NO.	FIG.
11-26-79	S.F.	CEPS-X-303	14

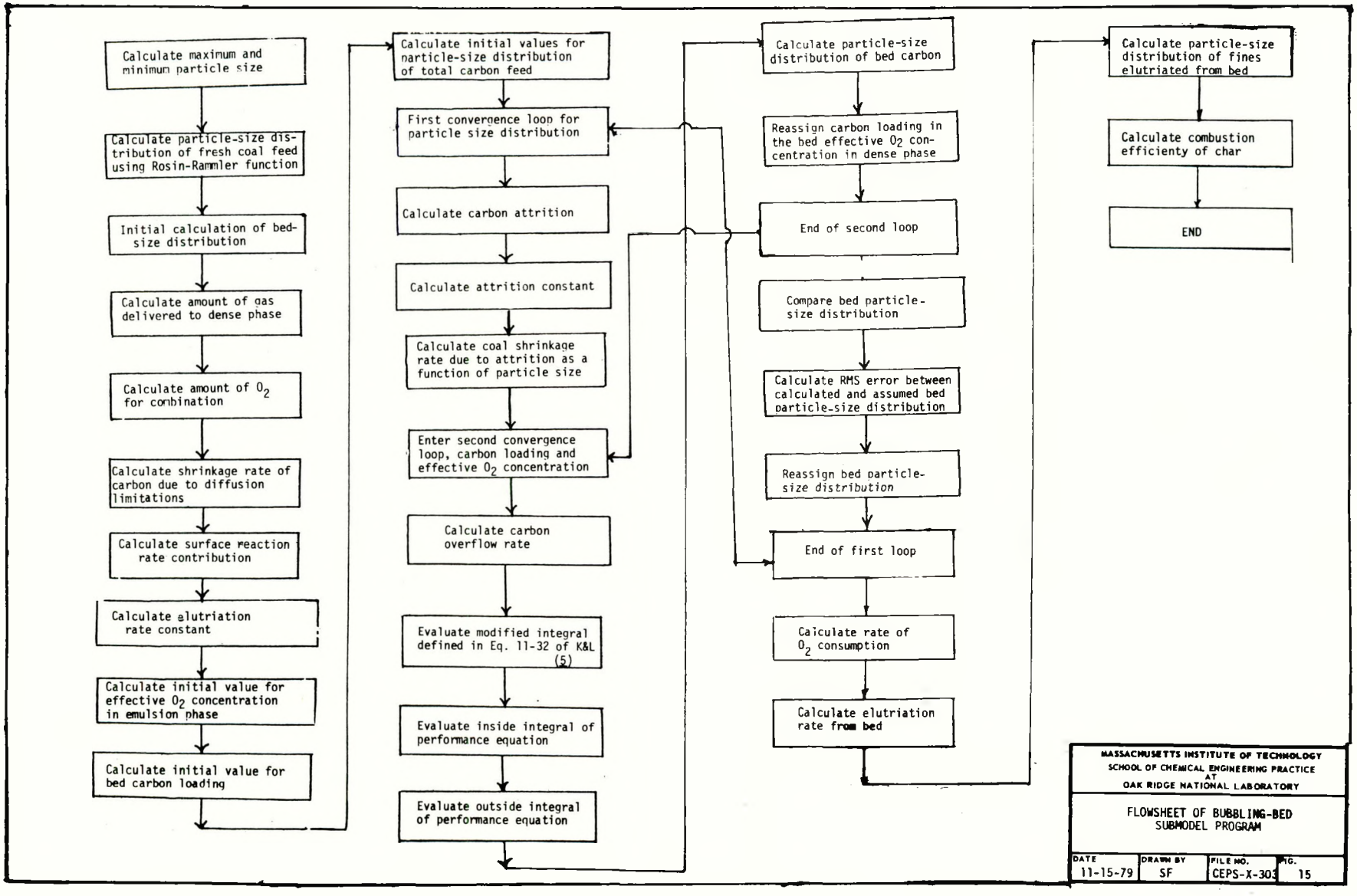
Calculate maximum and minimum particle size
Calculate particle-size distribution of fresh coal feed using Rosin-Rammler function
Initial calculation of bed-size distribution
Calculate amount of gas delivered to dense phase
Calculate amount of O_2 for combination
Calculate shrinkage rate of carbon due to diffusion limitations
Calculate surface reaction rate contribution
Calculate elutriation rate constant
Calculate initial value for effective O_2 concentration in emulsion phase
Calculate initial value for bed carbon loading
Calculate initial values for particle-size distribution of total carbon feed
First convergence loop for particle size distribution
Calculate carbon attrition
Calculate attrition constant
Calculate coal shrinkage rate due to attrition as a function of particle size
Enter second convergence loop, carbon loading and effective O_2 concentration
Calculate carbon overflow rate
Evaluate modified integral defined in Eq. 11-32 of K&L (5)
Evaluate inside integral of performance equation
Evaluate outside integral of performance equation
Calculate particle-size distribution of bed carbon
Reassign carbon loading in the bed effective O_2 concentration in dense phase
End of second loop
Compare bed particle-size distribution
Calculate RMS error between calculated and assumed bed particle-size distribution
Reassign bed particle-size distribution
End of first loop
Caiculate rate of O_2 consumption
Calculate elutriation rate from bed
Calculate particle-size distribution of fines elutriated from bed
Calculate combustion efficienty of char
END
MASSACHUSETTS INSTITUTE OF TECHNOLOGY
SCHOOL OF CHEMICAL ENGINEERING PRACTICE
AT
OAK RIDGE NATIONAL LABORATORY
FLOWSHEET OF BUBBLING-BED SUBMODEL PROGRAM
DATE 11-15-79
DRAWN BY SF
FILE NO. CEPS-X-303
FIG. 15

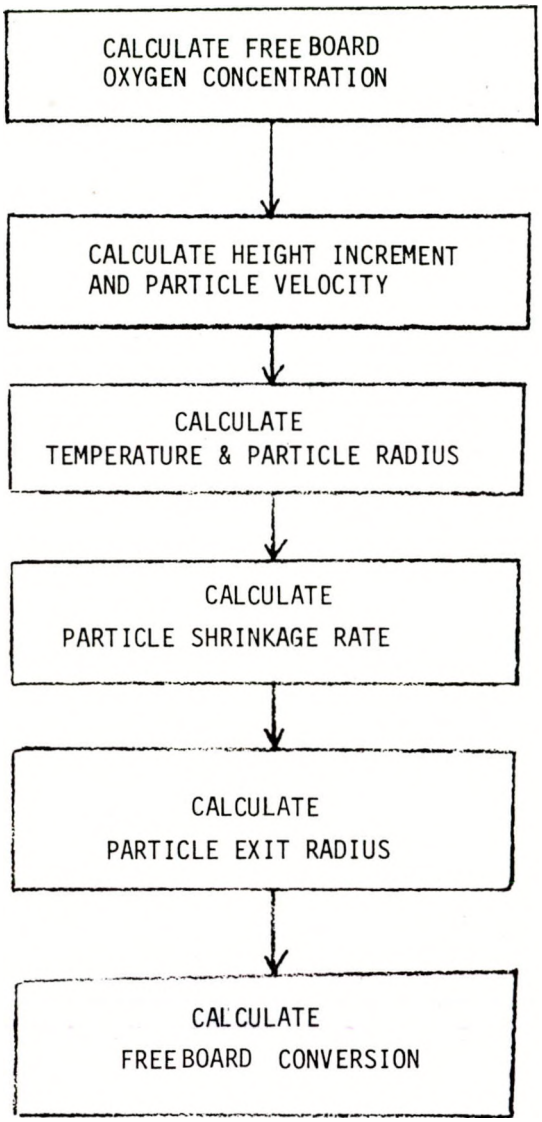

MASSACHUSETTS INSTITUTE OF TECHNOLOGY
SCHOOL OF CHEMICAL ENGINEERING PRACTICE
AT
OAK RIDGE NATIONAL LABORATORY

FLOWSHEET OF FREEBOARD SUBMODEL PROGRAM

DATE	DRAWN BY	FILE NO.	FIG.
11-27-79	S.F.	CEPS-X-303	16

7.4.2 Program Listing

```
00100   C*****************************************************************
00200   C
00300   C       MAIN PROGRAM FOR SIMULATION OF AN ATMOSPHERIC
00400   C       FLUIDIZED BED COAL COMBUSTOR
00500   C
00600   C*****************************************************************
00700   C
00800   C       INITIALIZE COMMON VARIABLES
00900   C
01000           COMMON /INPUT/ AIRF,COALF,COVFL
01100           COMMON /COAL/ XC,XS,XH,XO
01200           COMMON /TRANS/ R(61),PE(61),DELTR,ELTOT
01300   C
01400   C       CALL BUBBLING BED SUBROUTINE
01500   C
01600   1       CALL BUBED
01700   C
01800   C       CALL FREEBOARD SUBROUTINE
01900   C
02000   C
02100           CALL FB(XFB)
02200   C
02300   C       CALCULATE THE COMBUSTION EFFICIENCY
02400   C
02500           COMEF=(COALF*(XC+XS+XH-XO/8.)-ELTOT*XFB-COVFL)
02600        1          /COALF/(XC+XS+XH-XO/8.)
02700   C
02800   C       OUTPUT COMBUSTION EFFICIENCY
02900   C
03000           WRITE(5,10) COMEF
03100   10      FORMAT(E15.4)
03200           STOP
03300           END
03400   C*****************************************************************
03500   C
03600   C
03700   C       INTEGRATION SUBROUTINE--TRAPEZOIDAL RULE
03800   C
03900   C*****************************************************************
04000   C
04100           SUBROUTINE TRAP(FUNCT,DELTR,AAA,BBB,OUT)
04200           DIMENSION FUNCT(100)
04300           MIN=AAA
04400           MIN=MIN+1
04500           MAX=BBB
04600           SUM=0.
04700           MM=MAX-1
04800           DO 1 I=MIN,MAX
04900   1       SUM=SUM+FUNCT(I)
05000           OUT=DELTR/2.*(FUNCT(MIN)+2.*SUM+FUNCT(MAX))
        *
```

```
P
05000            OUT=DELTR/2.*(FUNCT(MIN)+2.*SUM+FUNCT(MAX))
05100            RETURN
05200            END
05300    C
05400    C
05500    C*********************************************************************
05600    C
05700    C        BUBBLING BED SUBROUTINE
05800    C
05900    C*********************************************************************
06000    C
06100    C
06200    C        DIMENSION AND COMMON INITIALIZATION
06300    C
06400            SUBROUTINE BUBED
06500            REAL LATRI,MU,IRM(61),KBP
06600            DIMENSION SC(61),FR(61),SA(61),FUNCT(61),EL(61),
06700           1  CELUT(61),WC(61),PBC(61),SH(61),CS(61),
06800           2  PF(61),PB(61),QPF(61),QPE(61),QPB(61)
06900    C
07000            COMMON /INPUT/AIRF,COALF, COVFL
07100            COMMON /DIST/ ROS1,ROS2
07200            COMMON /FBCP/BEDH,BEDA,TGAS,WIERT
07300            COMMON /PHYS/ RHOA,RHOC,RHOM,RHOG,DG,MU
07400            COMMON /COAL/ XC,XS,XH,XO
07500            COMMON /AIR/ UO,UMF,EXAIR,EMFLOW,CLFLOW,BUFLOW
07600            COMMON /BUB/ KBP,EMF,HT
07700            COMMON /MISC/ ATRIT,ACPTE
07800            COMMON /TRANS/R(61),PE(61),DELTR,ELTOT
07900    C
08000    C        SET INITIAL CONVERGENCE TOLERANCE AND CALCULATION CODE
08100    C
08200            TOLER=100.
08300            CODJIM=-123456.
08400    C
08500    C        CALCULATE INITIAL GAS VELOCITY AND OXYGEN CONCENTRATION
08600    C
08700            UF=UMF
08800            COIN=.21*RHOM
08900            COE=COIN*EXAIR/(1.+EXAIR)
09000    C
09100    C        CALCULATE MINIMUM AND MAXIMUM PARTICLE RADII
09200    C
09300            RMIN=.005*ROS2
09400            RMAX=2.*ROS2
09500    C
09600    C        CALCULATE PARTICLE RADII
09700    C
09800            DELTR=(RMAX-RMIN)/60.
09900            R(1)=RMIN
*
```

```
P
09900            R(1)=RMIN
10000            R(61)=RMAX
10100            DO 1 I=2,60
10200    1       R(I)=R(I-1)+DELTR
10300    C
10400    C       CALCULATE COAL FEED PARTICLE SIZE DISTRIBUTION
10500    C
10600            DO 2 I1=1,61
10700    2       PF(I1)=EXP(-(R(I1)/ROS2)**ROS1)*ROS1*R(I1)**(ROS1-1.)/
10800          1 ROS2**ROS1
10900    C
11000    C       CALCULATE INITIAL BED DISTRIBUTION
11100            DO 3 I2=1,61
11200    C
11300    3       PB(I2)=PF(I2)
11400    C
11500    C       CALCULATE OXYGEN AVAILABLE FOR COMBUSTION
11600    C
11700            TERM=-KBP*BEDH/UF
11800            IF (TERM+20.) 6,6,7
11900    7       TERM=EXP(TERM)
12000            GOTO 8
12100    6       TERM=0.
12200    8       FLOW=EMFLOW+CLFLOW+BUFLOW*(1-TERM)
12300    C
12400    C       CALCULATE CARBON SHRINKAGE RATE
12500    C
12600            C1=DG/RHOC
12700    C
12800    C       CALCULATE SCHMIDT NUMBER
12900    C
13000            SCH=MU/PHOM/28.84/DG
13100    C
13200    C       CALCULATE PARTICLE SURFACE TEMPERATURE AND
13300    C       REACTION RATE CONSTANT
13400    C
13500            TCHAR=TGAS+100.
13600            XKS=8710.*EXP(-35700./1.987/TCHAR)
13700            DO 9 J6=1,61
13800    C
13900    C       CALCULATE REYNOLDS NUMBER, SHERWOOD NUMBER, AND
14000    C       SHRINKAGE RATE
14100    C
14200            REY=RHOM*28.84*UF*R(J6)*2./MU
14300            SH(J6)=2.+.6*REY**.5*SCH**.3
14400            SC(J6)=C1/R(J6)*SH(J6)/2.*(XC+XS+XH-XO/8.)/
14500          1 (XC/12.+XS/32.+XH/4.-XO/32.)
14600    C
14700    C       CALCULATE RELATIVE RATES OF REACTION AND DIFFUSION
14800    C
*
```

```
P
14800    C
14900    9        CS(J6)=1./(1.+(XKS*TCHAR*R(J6)*1.3677E-1)/
15000          1  SH(J6)/DG)
15100    C
15200    C        CALCULATE ELUTRIATION RATE CONSTANT FROM
15300    C        HIGHLEY-MERRICK CORRELATION
15400    C
15500    C        CALCULATE PARTICLE TERMINAL VELOCITY AS
15600    C        FUNCTION OF RADIUS
15700    C
15800             DO 16 J5=1,61
15900             RCOM=.5*(90.7*MU)**.667/(RHOG*RHOC)**.333
16000             IF (RCOM-R(J5)) 17,18,18
16100    18       UT=1.195*(RHOC**2./RHOG/MU)**.333*2.*R(J5)
16200             GOTO 19
16300    17       RCOM=.289*MU**.667/(RHOG*RHOC)**.333
16400             IF (RCOM-R(J5)) 20,21,21
16500    21       UT=1.19*RHOC**.667/RHOG**.333/MU**.333*2.*R(J5)
16600             GOTO 19
16700    20       UT=.5444*RHOC*4.*R(J5)**2./MU
16800    19       CONTINUE
16900             CELUT(J5)=(130.*AIRF*EXP(-10.4*(UT/UO)**.5*
17000          1  (UMF/(UO-UMF))**.25*28.84/BEDA))
17100    16       CONTINUE
17200    C
17300    C        CALCULATE INITIAL BED CARBON LOADING
17400    C
17500             WCOAL=WIERT*.01
17600             IF (CODJIM.GT.0.) WCOAL=.875*COALF*XC*RHOC*ROS2**2./
17700          1  6./DG/COIN/3.*EXAIR
17800    C
17900    C        ENTER BED DISTRIBUTION CONVERGENCE LOOP
18000    C
18100             ICC=0
18200    4        CONTINUE
18300             ICC=ICC+1
18400    C
18500    C        CALCULATE CARBON ATTRITION FROM HIGHLEY-MERRICK
18600    C        CORRELATION
18700    C
18800             FR(1)=PB(1)*DELTR
18900             FR(2)=(PB(1)+PB(2))*DELTR
19000             DO 10 J1=1,61
19100             IF (J1-2) 15,15,11
19200    11       CALL TRAP(PB,DELTR,1.,61.,FR(J1))
19300    15       FUNCT(J1)=FR(J1)*PB(J1)
19400    10       CONTINUE
19500             CALL TRAP(FUNCT,DELTR,1.,61.,C2)
19600             LATRI=ATRIT/C2
19700             DO 14 J4=1,61
*
```

```
P
19700             DO 14 J4=1,61
19800    14       SA(J4)=LATRI/3.*FR(J4)*(UO-UMF)*R(J4)
19900             ICI=0
20000    C
20100    C        ENTER CARBON LOADING AND OXYGEN CONCENTRATION
20200    C        CONVERGENCE LOOP
20300    C
20400    34       CONTINUE
20500    C
20600    C        CALCULATE CARBON OVERFLOW RATE
20700    C
20800             ICI=ICI+1
20900             IF (WCOAL/WIERT-.9) 60,61,61
21000    61       COVFL=ACPTE*WCOAL/(.1*WIERT)
21100             GOTO 62
21200    60       COVFL=WCOAL*ACPTE/(WIERT-WCOAL)
21300    62       CONTINUE
21400    C
21500    C        EVALUATE KUNII & LEVENSPIEL I-INTEGRAL (EQN 11.32)
21600    C
21700             DO 22 K2=1,61
21800             FUNCT(K2)=(COVFL/WCOAL+CELUT(K2)*BEDA/WIERT*RHOA/RHOC+
21900          ▸ 1  3.*SC(K2)*COE*(1.-CS(K2))/R(K2))/(SC(K2)*COE*(1.-CS(K2))
22000            2  +SA(K2))
22100    22       CONTINUE
22200             DO 23 K3=1,58
22300             AK3=K3
22400             CALL TRAP(FUNCT,DELTR,AK3,61.,RIRM)
22500             IF (RIRM-170.) 59,64,64
22600    64       RIRM=170.
22700    59       CONTINUE
22800             IRM(K3)=EXP(-RIRM)
22900    23       CONTINUE
23000             RIR59=(FUNCT(59)+FUNCT(60)+FUNCT(61))*DELTR
23100             RIR60=(FUNCT(60)+FUNCT(61))*DELTR
23200             IF (RIR59.GT.150.) RIR59=150.
23300             IF (RIR60.GT.150.) RIR60=150.
23400             IRM(59)=EXP(-RIR59)
23500             IRM(60)=EXP(-RIR60)
23600             IRM(61)=1.
23700             DO 57 M7=1,61
23800             IF (IRM(M7)-1.E-20) 58,57,57
23900    58       IRM(M7)=1.E-20
24000    57       CONTINUE
24100    C
24200    C        EVALUATE INSIDE OF KUNII & LEVENSPIEL INTEGRAL 11.38
24300    C
24400             DO 24 K4=1,61
24500             IF (K4-28) 26,26,27
24600    26       DO 25 K5=K4,61
*
```

```
P
24600    26       DO 25 K5=K4,61
24700             FUNCT(K5)=PF(K5)/IRM(K5)
24800    25       CONTINUE
24900             AK4=K4
25000             CALL TRAP(FUNCT,DELTR,AK4,61.,DINT)
25100             GOTO 30
25200    C
25300    C        EVALUATE OUTSIDE OF KUNII & LEVENSPIEL INTEGRAL 11.38
25400    C
25500    27       DINT=0.
25600             IF (K4.EQ.61) GOTO 30
25700             DO 31 L1=K4,60
25800    31       DINT=DINT+PF(L1)/IRM(L1)*DELTR
25900    30       CONTINUE
26000             WC(K4)=COALF*(XC+XH+XS+XO/8.)*IRM(K4)/ABS(SC(K4)
26100         1    *COE*(1.-CS(K4))+SA(K4))*DINT
26200    24       CONTINUE
26300             CALL TRAP(WC,DELTR,1.,61.,WCOLC)
26400    C
26500    C        CALCULATE CARBON PARTICLE SIZE DISTRIBUTION
26600    C
26700             DO 35 L5=1,61
26800    35       PBC(L5)=WC(L5)/WCOLC
26900             PBC(61)=1.E-5
27000             PBINT=0
27100             DO 5 I5=1,61
27200             FUNCT(I5)=PBC(I5)/R(I5)**2.*(1.-CS(I5))*SH(I5)
27300     5        CONTINUE
27400             CALL TRAP(FUNCT,DELTR,1.,61.,PBINT)
27500    C
27600    C        TEST FOR CARBON LOADING CONVERGENCE
27700    C
27800             IF (ICI-200)42,42,32
27900    43       WRITE(5,100)
28000             BOMB=1.
28100    42       DIF=(WCOLC-WCOAL)/WCOAL
28200             IF(ABS(DIF)-.001*TOLER)32,32,33
28300    33       CONTINUE
28400    C
28500    C        RECALCULATE CARBON LOADING AND OXYGEN CONCENTRATION
28600    C
28700              WCOAL=WCOLC*(1.+DIF)
28800             COE=COIN/((1.5*WCOAL/(FLOW/C1/PBINT))+1.)
28900             IF(CODJIM.GT.0.)GO TO 999
29000             SBEDH=WIERT/RHOA/BEDA/(1.-EMF)
29100             DWC=WCOAL/BEDA/SBEDH
29200             HST=UO/(1.5*C1*DWC*PBINT)
29300             TER=HT/HST*(1.-DELPL)
29400             IF(TER.GE.140.)TER=140.
29500             CPT=COIN*EXP(-TER)
*
```

```
P
29500            CPT=COIN*EXP(-TER)
29600            COEN=CPT/(1.+(BEDH-HT)/HST*UO/FLOW*(1.-DELB))
29700             TERR=(1.-DELPL)*HT/HST
29800            IF (TERR.GT.140.)TERR=140.
29900            COE=COIN/(1.-DELPL)*HST/BEDH*(1.-EXP(-TERR))
30000          1 +COEN*(1.-HT/BEDH)
30100    999     CONTINUE
30200            GO TO 34
30300    32      CONTINUE
30400    C
30500    C       CHECK BED DISTRIBUTION CONVERGENCE
30600    C
30700            PB(61)=1.E-5
30800            ERR=0.
30900            TOLER=1.
31000            DO 40 M1=1,61
31100            IF(PB(M1)-PBC(M1))65,65,66
31200    65      PL=PB(M1)
31300            GO TO 400
31400    66      PL=PBC(M1)
31500    C
31600    C       CALCULATE DIFFERENCE BETWEEN CALCULATED AND ASSUMED
31700    C       BED SIZE DISTRIBUTION
31800    C
31900    400     ERROR1=((PB(M1)-PBC(M1))/PL)**2
32000            IF(PB(M1).LE.1.E-4.AND.PBC(M1).LE.1.E-4)ERROR1=0.
32100    40      ERR=ERR+ERROR1
32200            ERAVG=SQRT(ERR)/61.
32300    C
32400    C       CHECK SECOND LOOP COUNTER
32500    C
32600            IF(ICC-200)44,44,45
32700    45      WRITE(NWRIT,101)
32800            BOMB=1.
32900    C
33000    C       TEST FOR CONVERGENCE OF BED PARTICLE SIZE DISTRIBUTION
33100    C
33200    44      IF(ERAVG-.001)36,36,37
33300    37      CONTINUE
33400    C
33500    C       REASSIGN BED PARTICLE SIZE DISTRIBUTION
33600    C
33700            DO 38 L8=1,61
33800    38      PB(L8)=PBC(L8)
33900            DO 53 M8=1,61
34000            IF(PB(M8)-1.E-10)54,53,53
34100    54      PB(M8)=1.E-10
34200    53      CONTINUE
34300            GO TO 4
34400    C
*
```

```
P
34400    C
34500    C
34600    C        END OF BED PARTICLE SIZE DISTRIBUTION LOOP
34700    C
34800    36       CONTINUE
34900    C
35000    C        CALCULATE THE RATE OF OXYGEN CONSUMPTION
35100    C
35200             COCON=FLOW*(CPT-COEN)*BEDA+UO*BEDA*(COIN-CPT)
35300    C
35400    C         CALCULATE ELUTRIATION RATE FROM BED
35500    C
35600             ELTOT=0.0
35700             DO 56 M6=1,61
35800    56       EL(M6)=CELUT(M6)*BEDA*WC(M6)/WIERT*RHOA/RHOC
35900              CALL TRAP(EL,DELTR,1.,61.,ELTOT)
36000    C
36100    C        CALCULATE ELUTRIANT PARTICLE SIZE DISTRIBUTION
36200    C
36300              DO 41 I1=1,61
36400             IF(ELTOT)186,186,187
36500    186      PE(I1)=0.0
36600             GO TO 41
36700    187      PE(I1)=EL(I1)/ELTOT
36800    41       CONTINUE
36900    C
37000    C        CALCULATE AVERAGE PARTICLE RADIUS FOR FEED, BED,
37100    C        AND ELUTRIANT
37200    C
37300             DO 1717 JJ=1,61
37400             QPF(JJ)=R(JJ)*PF(JJ)
37500             QPE(JJ)=R(JJ)*PE(JJ)
37600    1717     QPB(JJ)=R(JJ)*PB(JJ)
37700             CALL TRAP (PF,DELTR,1.,61.,PFSM)
37800             CALL TRAP (PE,DELTR,1.,61.,PESM)
37900             CALL TRAP (PB,DELTR,1.,61.,PBSM)
38000             CALL TRAP (QPF,DELTR,1.,61.,FAV)
38100             CALL TRAP (QPE,DELTR,1.,61.,EAV)
38200             CALL TRAP (QPB,DELTR,1.,61.,BAV)
38300             FAV=FAV/PFSM
38400             EAV=EAV/PESM
38500             BAV=BAV/PBSM
38600    C
38700    C        FORMAT SECTION FOR ERROR MESSAGES
38800    C
38900    100      FORMAT(10X,'COMB:INNER LOOP NOT CONVERGING')
39000     101      FORMAT(10X,'COMB:MIDDLE LOOP NOT CONVERGING')
39100              RETURN
39200             END
39300    C
*
```

```
P
39300    C
39400    C*****************************************************************
39500    C
39600    C       FREEBOARD SIMULATION SUBROUTINE
39700    C
39800    C*****************************************************************
39900            SUBROUTINE FB(XFB)
40000    C
40100    C       DIMENSION AND COMMON INITIALIZATION
40200    C
40300            DIMENSION R(100),SC(100),RTOP(61),FNRT(61)
40400            REAL MU
40500            COMMON /PHYS/RHOA,RHOC,RHOM,RHOG,DG,MU
40600            COMMON /AIR/ UO,UMF,EXAIR,EMFLOW,CLFLOW,BUFLOW
40700            COMMON /COAL/ XC,XS,XH,XO
40800            COMMON /FBD/ TOUT,HFB,FRACV
40900            COMMON /FBCP/ BEDH,BEDA,TBED,WIERT
41000            COMMON /TRANS/ RO(61),PE(61),DELTR,ELTOT
41100    C
41200    C       CALCULATE FREEBOARD OXYGEN CONCENTRATION
41300    C
41400            COIN=.21*RHOM
41500            COE=COIN*EXAIR/(1.+EXAIR)
41600    C       CALCULATE HEIGHT INCREMENT AND PARTICLE VELOCITY
41700            DX=HFB/100.
41800    C
41900            X=0.
42000            V=FRACV*UO
42100    C
42200    C       ENTER FIRST INTEGRATION LOOP
42300    C
42400            DO 99 K=1,61
42500            FNRT(K)=0.
42600            IF (RO(K).LE.0.) GOTO 99
42700            DO 10 J=1,100
42800    10      SC(J)=0.
42900            R(1)=RO(K)
43000    C
43100    C       ENTER INNER INTEGRATION LOOP
43200    C
43300            DO 999 I=1,99
43400    C
43500    C       CALCULATE HEIGHT, TEMPERATURE, SCHMIDT NUMBER, SHERWOOD
43600    C       NUMBER, AND REYNOLDS NUMBER
43700    C
43800            X=X+DX
43900            T=TBED+(TOUT-TBED)/HFB*X
44000            SCH=MU/(RHOM*28.84*DG)
44100            REY=RHOM*28.84*UO*R(I)*2./MU
44200            SH=2.+.6*REY**.5*SCH**.333
*
```

```
P
44200           SH=2.+.6*REY**.5*SCH**.333
44300           SR=DG/RHOC/R(I)*SH/2.*(XC+XS+XH-XO/8.)
44400         1   /(XC/12.+XS/32.+XH/4.-XO/32.)
44500     C
44600     C       CALCULATE PARTICLE SHRINKAGE RATE
44700     C
44800           XKS=8710.*EXP(-35700./1.987/(T+100.))
44900           CS=1./(1.+(XKS*(T+100.)*R(I)*1.3677E-1)/SH/DG)
45000           SC(I)=SR*COE*(1.-CS)
45100           AI=I
45200     C
45300     C       EVALUATE INNER INTEGRAL
45400     C
45500           CALL TRAP(SC,DX,1.,AI,AINT)
45600           R(I+1)=R(I)-AINT/V
45700     999   CONTINUE
45800     C
45900     C       CALCULATE EXIT PARTICLE SIZE
46000     C
46100           IF (R(100).LE.0.) R(100)=0.
46200           RTOP(K)=R(100)
46300     C
46400     C       EVALUATE OUTER INTEGRAL AND CALCULATE XFB
46500     C
46600           FNRT(K)=(R(100)/R(1))**3.*PE(K)
46700     99    CONTINUE
46800           CALL TRAP(FNRT,DELTR,1.,61.,XFB)
46900           IF (XFB.GT.1.) XFB=0.
47000           RETURN
47100           END
47200     C*****************************************************************
47300     C
47400     C       THIS SUBROUTINE PROVIDES THE INITIAL VALUES FOR
47500     C       ALL THE INPUT PARAMETERS SPECIFIED IN COMMON
47600     C
47700     C*****************************************************************
47800     C
47900           SUBROUTINE BLKDA
48000           BLOCK DATA
48100     C
48200           REAL MU,KBP
48300           COMMON /INPUT/ AIRF,COALF,COVFL
48400           COMMON /DIST/ ROS1,ROS2
48500           COMMON /FBCP/ BEDH,BEDA,TGAS,WIERT
48600           COMMON /PHYS/ RHOA,RHOC,RHOM,RHOG,DG,MU
48700           COMMON /COAL/ XC,XS,XH,XO
48800           COMMON /AIR/ UO,UMF,EXAIR,EMFLOW,CLFLOW,BUFLOW
48900           COMMON /BUB/ KBP,EMF,HT
49000           COMMON /MISC/ ATRIT,ACPTE
49100           COMMON /FBD/ TOUT,HFB,FRACV
*
```

```
P
49100            COMMON /FBD/ TOUT,HFB,FRACV
49200   C
49300            DATA AIRF,COALF/2.264,1.084/
49400            DATA ROS1,ROS2/1.068,6.E-4/
49500            DATA BEDH,BEDA,TGAS,WIERT/1.22,3.3445,1144.,3500./
49600            DATA RHOA,RHOC,RHOM,RHOG,DG,MU
49700           1      /2363.,1522.,1.07E-2,.3094,2.E-4,4.56E-2/
49800            DATA XC,XS,XH,XO/.6953,.0309,.0497,.0778/
49900            DATA UO,UMF,EXAIR,EMFLOW,CLFLOW,BUFLOW
50000           1      /2.5,.7422,.18,2.6E-2,1.7E-2,2.29/
50100            DATA KBP,EMF,HT/29.41,.45,.05/
50200            DATA ATRIT,ACPTE/.005,.16/
50300            DATA TOUT,HFB/1300.,3./
50400            DATA FRACV/.6/
50500   C
50600   C
50700            RETURN
50800            END
◆
```

7.5 Nomenclature

A	bed cross-sectional area, m^2
A_o	pre-exponential factor, g/cm^2-s-kPa
b	Rosin-Rammler parameter
B	parameter used in Sect. 7.3.2
C	parameter used in Sect. 7.3.2
C_p	bulk emulsion-phase oxygen concentration, mol/m^3
C_s	surface oxygen concentration, mol/m^3
d_b	bubble diameter, m
d_p	acceptor particle diameter, m
D	gas diffusivity, m^2/s
E	activation energy, J/mol
F_a	air flow rate, mol/s
F_o	coal feed rate, kg/s
F_1	coal overflow rate, kg/s
F_2	coal elutriation rate, kg/s
g	gravitational acceleration, m/s^2
G	parameter used in Sect. 7.3.2
$I(r,r_o)$	performance equation integral defined in Eq. (5)
K_a	attrition constant
K_s	combustion reaction-rate constant, g/cm^2-s-kPa
$K(r)$	elutriation-rate constant, kg/m^2-s
n	Rosin-Rammler parameter
N	moles of carbon
P	reactor pressure, Pa
$p_b(r)$	bed particle-size distribution

$p_e(r_o)$	elutriant particle-size distribution
$p_o(r)$	feed particle-size distribution
$p_1(r)$	overflow particle-size distribution
$P_o(r)$	weight fraction of feed with particle size less than r
r	particle radius, m
r_o	particle radius entering freeboard, m
r_f	particle radius at top of freeboard, m
R	ideal gas constant, 1.987 J/mol-K
R(r)	particle shrinkage rate, μm/s
Re	Reynolds number, dimensionless
Sc	Schmidt number, dimensionless
Sh	Sherwood number, dimensionless
$S_a(r)$	shrinkage rate due to attrition, μm/s
$S_c(r)$	shrinkage rate due to combustion, μm/s
$S_t(r)$	total shrinkage rate, μm/s
t	time, s
T	temperature, K
u_{mf}	minimum fluidization velocity, m/s
u_o	superficial velocity, m/s
u_t	terminal velocity, m/s
v	particle velocity in freeboard, m/s
W	bed weight, kg
x	axial coordinate in freeboard, m
x_f	total freeboard height, m

Greek Symbols

β	parameter in calculating u_{mf}
ε_{mf}	void fraction in emulsion phase
μ	gas viscosity, N-s/m^2
η_c	combustion efficiency
ν	particle-size density function
ϕ_s	particle sphericity
ρ_c	coal apparent density, kg/m^2
ρ_g	mass density of air feed, kg/m^3
ρ_m	molar density of air feed, kg-mol/m^3
ξ_{fb}	conversion in freeboard

7.6 Program Variables

Input Variables

ATRET	Attrition constant	
ACPTE	Acceptor effluent rate	kg/s
BEDA	Bed cross-sectional area	m^2
BEDH	Expanded bed height	m
BUFLOW	Air flow in bubble phase	kg mol/s
CLFLOW	Transport air flow rate	kg mol/s
COIN	Oxygen concentration in incoming air	kg mol/m^3
DG	Gas diffusivity	m^2/s
EMF	Void fraction in emulsion phase	
EMFLOW	Air flow rate in emulsion phase	kg mol/s
HT	Transition height	m
KBP	Mass exchange coefficient between bubble and emulsion phase	s^{-1}

MU	Gas viscosity	$N\text{-}s/m^2$
RHOA	Acceptor density in bed	kg/m^3
RHOC	Coal apparent density	kg/m^3
RHOG	Mass density of incoming air	kg/m^3
RHOM	Molar density of incoming air	$kg\ mol/m^3$
ROS1	Rosin-Rammler function parameter	
ROS2	Coal mean particle radius	cm
TGAS	Bed temperature	K
TOLER	Tolerance limit in convergence loop	
UO	Superficial velocity	m/s
UF	Fluidizing gas velocity	m/s
UMF	Minimum fluidization velocity	m/s
WIERT	Weight of inert in bed	kg
XC	Weight fraction of carbon in coal	
XH	Weight fraction hydrogen in coal	
XS	Weight fraction sulfur in coal	
XO	Weight fraction oxygen in coal	

Output Variables

COE	Effective oxygen concentration in emulsion phase	$kg\ mol/m^3$
CELUT	Elutriation rate constant	$kg/s\text{-}m^2$
COCON	Oxygen consumption rate	kg mol/s
CS	Surface oxygen concentration	$kg\ mol/m^3$
COVFL	Carbon overflow rate	kg/s
COMEF	Combustion efficiency	
ELTOT	Elutriation rate	kg/s
LATRIT	Attrition constant	

PF	Coal particle-size distribution of feed	
PE	Coal particle-size distribution of elutriants	
PB	Coal particle-size distribution of bed	
SA	Coal shrinkage rate due to attrition	m/s
SC	Shrinkage rate of carbon due to diffusion limited	m/s
UT	Terminal velocity	m/s
WCOAL	Carbon loading in bed	kg
XKS	Surface reaction rate	mol/m^2-s

7.7 Literature References

1. Babcock & Wilcox Co., "Fluidized Bed Combustion Development Facility and Commercial Utility AFBC Design Assessment," EPRI Contract RP-718-2, June 1979.

2. Baron, R.E., J.M. Beer, G. Borghi, J.L. Hodges, and A.F. Sarofim, "A Model of Coal Combustion in Fluidized Bed Combustors," Dept. of Chemical Engineering, Mass. Institute of Technology, Cambridge, MA.

3. Beer, J.M., H.A. Becker, and B.M. Gibbs, "A Model for Fluidized-Bed Combustion of Coal," Institute of Fuel Symposium Series No. 1, p. A1-1 to A1-10.

4. Horio, M., S. Mori, and I. Muchi, "A Model Study for the Development of Low NO_x Fluidized-Bed Coal Combustors," Dept. of Iron and Steel Engineering, Nagoya University, Japan.

5. Kunii, D., and O. Levenspiel, Fluidized Engineering, Chapts. 10-11, Wiley, New York, 1969.

6. Louis, J.F., and S.E. Tung, *et al.* "A First Order System Model of Fluidized Bed Combustors," MIT Energy Laboratory, Vol. 1, Cambridge, MA, February 1978.

7. Merrick, D., and J. Highley, "Particle Size Reduction and Elutriation in a Fluidized Bed Process," AIChE Symp. Series, 70(137), 366 (1971).

8. Sharma, P.K., "Application of MIT Combustion Submodel to TVA Coal," Energy Laboratory, Mass. Institute of Technology, Cambridge, MA, May 1979.

9. Yates, J.G., and P.N. Rowe, "A Model for Chemical Reaction in the Freeboard Region Above a Fluidised Bed," Trans. Instn. Chem. Engrs., 55, 137 (1977).

ORNL/MIT-303

INTERNAL DISTRIBUTION

1. D.A. Canonico
2. H.D. Cochran, Jr.
3. J.R. Hightower
4. J.E. Jones, Jr., 9201-3
5-8. A.A. Khan
9. L.E. McNeese
10. G.E. Moore
11. T.W. Pickel
12. M.W. Rosenthal
13. M. Siman-Tov
14. J.W. Wells
15. W.R. Williams
16. R.G. Wymer
17-18. Central Research Library
19. Document Reference Section
20-22. Laboratory Records
23. Laboratory Records, ORNL R.C.
24. ORNL Patent Office
25-39. MIT Practice School, 1505

EXTERNAL DISTRIBUTION

40. J.M. Beer, MIT, Cambridge, MA
41. J.P. Longwell, MIT, Cambridge, MA
42. A.F. Sarofim, MIT, Cambridge, MA
43. S.M. Senkan, MIT, Cambridge, MA
44. S.E. Tung, MIT, Cambridge, MA
45. J.E. Vivian, MIT, Cambridge, MA
46. G.C. Williams, MIT, Cambridge, MA
47. H.M. Wood, MIT, GE, Selkirk, NY
48. Morgantown Energy Technology Center
P.O. Box 880, Morgantown, WV
49. Office Asst. Mgr., Energy R&D, DOE
50-76. Technical Information Center